DEUTSCHES ELEKTRONEN-SYNCHROTRON DESY

DESY 80/124
December 1980

NEW e^+e^- PHYSICS

by

B. H. Wiik

NOTKESTRASSE 85 · 2 HAMBURG 52

To be sure that your preprints are promptly included in the
HIGH ENERGY PHYSICS INDEX ,
send them to the following address (if possible by air mail) :

DESY
Bibliothek
Notkestrasse 85
2 Hamburg 52
Germany

DESY 80/124
December 1980

NEW e^+e^- PHYSICS

by

B.H.Wiik

Deutsches Elektronen-Synchrotron DESY, Hamburg, Germany.

Invited Talk given at the XXth International Conference on High Energy Physics, University of Wisconsin, Madison, Wisconsin, July 17 - 23, 1980.

NEW e^+e^- PHYSICS

B.H.Wiik

Deutsches Elektronen-Synchrotron DESY, Hamburg, Germany.

I. INTRODUCTION

In this talk I will review data obtained in e^+e^- collisions at PETRA during the past year using four large detectors, MARK J, JADE, PLUTO and TASSO. Each experiment has collected a total luminosity of about 5500 nb^{-1} at c.m. energies between 12 GeV and 36.6 GeV with the bulk of the luminosity ($\sim$ 4800 nb^{-1}) at energies above 30 GeV. This corresponds to some 2500 multihadron events per experiment. PLUTO was replaced by a new experiment CELLO early this year.

Several new results have been obtained during the past year: The data[1] on various QED reactions agree with the theory up to q^2 = 1000 GeV^2 and s = 1200 GeV^2. Lepton universality is valid down to distances of 2 x 10^{-16} cm. The cross sections for these reactions have been determined with a precision similar to the size of the effects expected from the electroweak interference terms. The experiments further show[2] that there is no new charged lepton with a mass less than 17 GeV.

Hadrons produced at high energies in e^+e^- annihilation appear in two nearly collinear jets. The charged multiplicity and the charged particle composition of the jets have been determined[3] for momenta up to 5-6 GeV/c and long range charge correlations[4] among the fast particles in the two jets have been observed for the first time. The data[2] also show that the threshold for $t\bar{t}$ production where t is a quark with charge 2/3e must be above 36.0 GeV.

The outstanding experimental result has been the observation[5-9] of three jet events. Such events are evidence for hard gluon bremsstrahlung which is expected to occur in any field theory of strong interactions. Using different methods each group[4,10-12] has observed on the order of 200 clear three jet events. An analysis of these events shows that the gluon is most likely a vector particle and there are first indications that quarks and gluons fragment differently. The strength of the coupling between quarks and gluons has been determined.

A wealth of new information on photon-photon collisions has been reported[13] to the Conference. From the collisions of two real photons there are, besides data on QED and resonance production, also results[14] on $\gamma\gamma \to \rho^0\rho^0$ [14] and on $\gamma\gamma \to$ hadrons. In the multihadron data there are evidence for two jet production as expected if the photon has a point-like component. Data on deep inelastic electron-photon scattering have also been reported for the first time.

In this talk I'll describe these results in more detail. A more complete discussion can be found in the minirapporteur talks on PETRA physics referenced above.

II. ELECTROWEAK REACTIONS

The Feynman graphs for Bhabha scattering, lepton pair production and two photon annihilation are shown in Fig. 1. Effects caused by

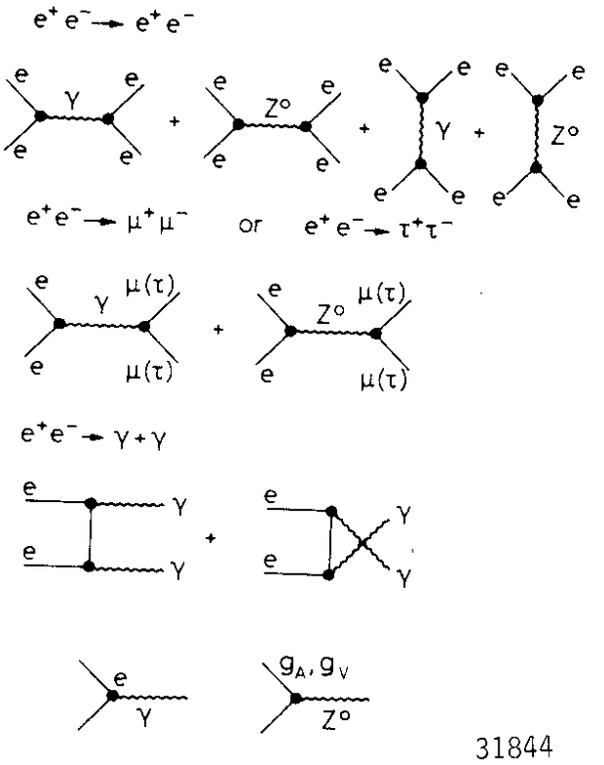

Fig. 1 - Feynman graphs for
a) $e^+e^- \to e^+e^-$
b) $e^+e^- \to \mu^+\mu^-(\tau^+\tau^-)$
c) $e^+e^- \to \gamma\,\gamma$

the interference of the weak and the electromagnetic currents start to become visible at the highest energies now available at PETRA and we will return to these effects after a brief discussion on QED limits.

II.1 TEST OF QED

The QED predictions are based on the validity of the Maxwell equations and on the assumption that leptons are pointlike objects without excited states. The reactions above make it possible to test these assumptions at very small distances in a clean environment with only small corrections due to strong interactions.

The standard procedure used to compare data with the QED predictions can be summarized as follows:
1) Weak effects are neglected.
2) The measured cross section $d\sigma_0/d\Omega$ is corrected[15] for radiative effects δ_R and effects due to the hadronic vacuum polarization δ_H.

$$\frac{d\sigma_c}{d\Omega} = \frac{d\sigma_0}{d\Omega}\,(1 + \delta_R + \delta_H). \qquad (1)$$

3) The corrected cross section is compared to the QED predicted cross section and deviations are parametrized[16] in terms of form factors. The formfactors used for Bhabha scattering and lepton pair production can be written as:

$$F_s(q^2) = 1 \mp \frac{q^2}{q^2 - \Lambda_{s\pm}^2} \qquad F_t(s) = 1 \mp \frac{s}{s - \Lambda_{t\pm}^2} \qquad (2)$$

where F_s and F_t are respectively the formfactors for spacelike and timelike momentum transfer squared.

The reaction $e^+e^- \to \gamma\gamma$ is modified by a form factor[17] of the type $F(q^2) \sim 1 \pm q^4/\Lambda_\pm^4$. Exchange of a heavy electronlike lepton would modify[18] the cross-section as

$$F(s) \sim 1 + (s^2/2\Lambda^4)\sin^2\theta \qquad (3)$$

where Λ is the mass of the heavy lepton.

All groups working at PETRA have data[2,19] on these reactions and some typical results are shown in Figs. 2-5.

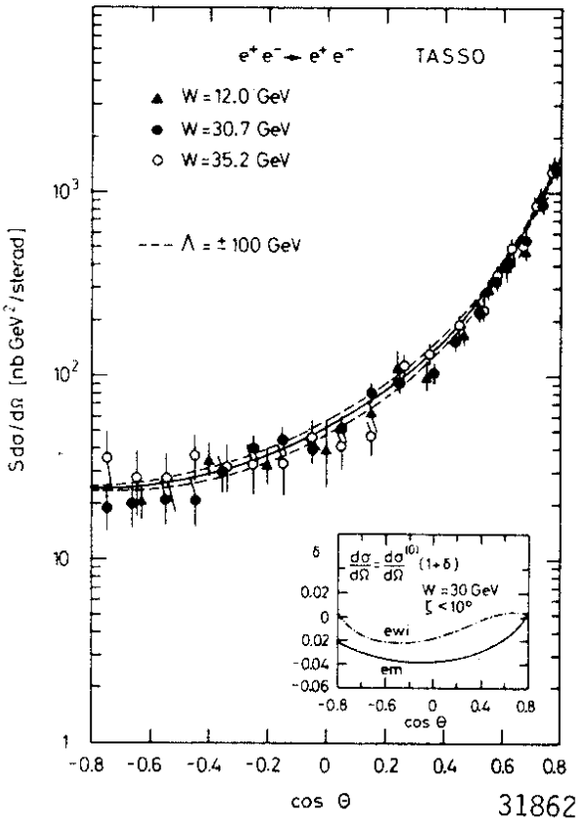

Fig. 2 - The cross section $s \cdot d\sigma/d\Omega$ for $e^+e^- \to e^+e^-$ measured by TASSO between 12.0 GeV and 35.2 GeV in c.m.

The cross section $s\, d\sigma/d\Omega(e^+e^- \to e^+e^-)$ measured by the TASSO Collaboration for c.m. energies between 12 and 35.2 GeV is plotted in Fig.2 versus scattering angle θ. The data scatter around the QED prediction shown as the solid curve, the dotted curve indicates the limits corresponding to a cut off parameter Λ = 100 GeV.

The total cross section for $e^+e^- \to \mu^+\mu^-$ measured by JADE, MARK J, PLUTO and TASSO is plotted in Fig. 3 versus c.m. energy. The data agree well with the QED prediction shown as the solid curve and they are in general within the dotted curves corresponding to a cutoff parameter Λ of 100 GeV.

The total cross section for $e^+e^- \to \tau^+\tau^-$ measured by MARK J, PLUTO and TASSO is plotted in Fig. 4 versus c.m. energy. This reaction has a very distinct signature at high energies and is easily separated from multihadron reactions. Again the data are in good agreement with the QED prediction shown as the solid curve.

The angular distribution for $s\, d\sigma/d\Omega$ $(e^+e^- \to \gamma\gamma)$ measured by the JADE and PLUTO Collaborations is plotted in Fig.5 for c.m. energies between 12 and 31.6 GeV. The data are in good agreement with the QED prediction, the deviation corresponding to a cutoff parameter Λ = 40 GeV is shown as the dotted curve.

The data are therefore in agreement with QED and the limits on Λ are summarized in Table 1.

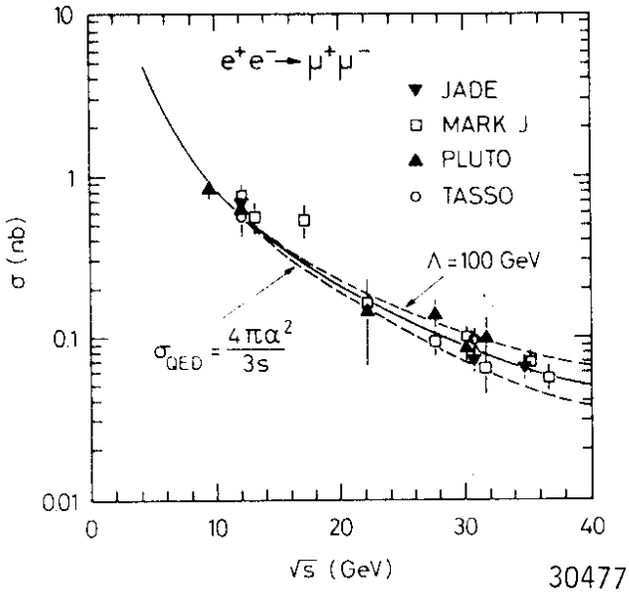

Fig. 3
The total cross section for $e^+e^- \to \mu^+\mu^-$ measured by JADE, MARK J, PLUTO and TASSO plotted versus c.m. energy.

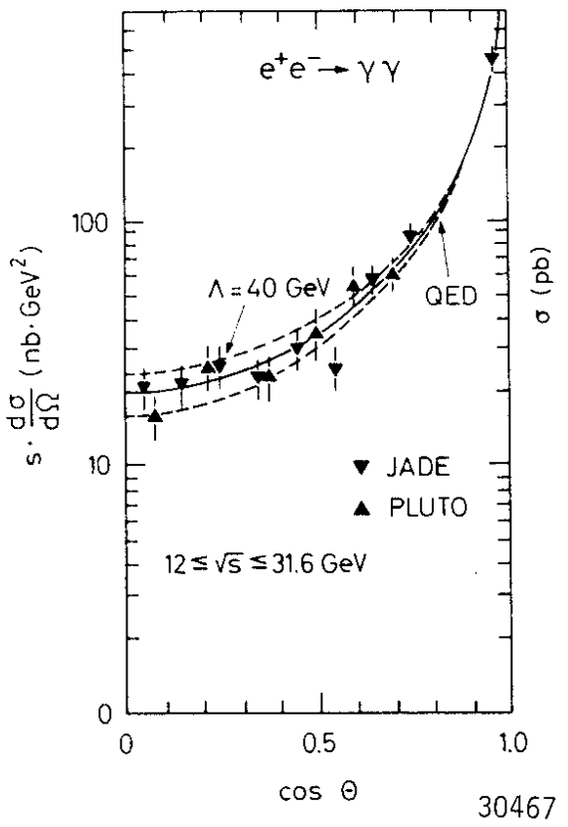

Fig. 5
The cross section $s\frac{d\sigma}{d\Omega}$ for $e^+e^- \to \gamma\gamma$ measured by JADE and PLUTO plotted versus cosθ.

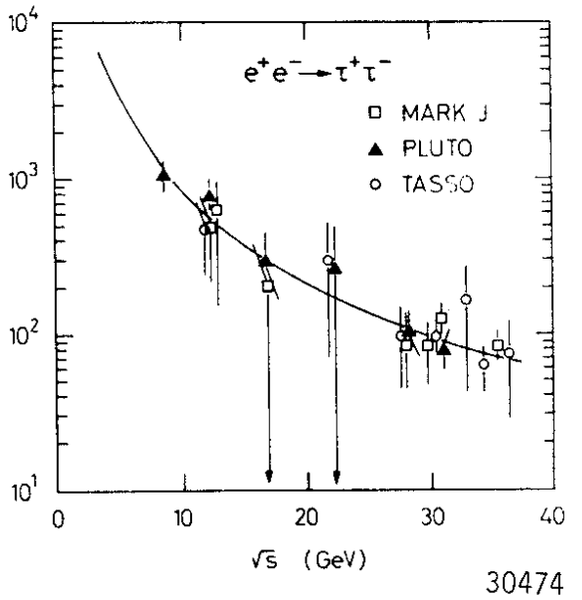

Fig. 4
The total cross section for $e^+e^- \to \tau^+\tau^-$ measured by MARK J, PLUTO and TASSO plotted versus c.m. energy.

Table 1 - Limits on $\Lambda_{\pm}$

	JADE	MARK J	PLUTO	TASSO
$e^+e^- \to e^+e^-$				
Λ_+	112	91	80	150
Λ_-	106	142	234	136
$e^+e^- \to \mu^+\mu^-$				
Λ_+	137	123	116	80
Λ_-	96	142	101	118
$e^+e^- \to \tau^+\tau^-$				
Λ_+	-	76	74	115
Λ_-	-	154	65	76
$e^+e^- \to \gamma\gamma$	$F(q^2) = 1 \pm q^4/\Lambda_{\pm}^4$			
Λ_+	-	44	46	-
Λ_-	-	34	36	-
	heavy electron Λ^*			
Λ_+	47	55	46	34
Λ_-	44	38	-	42

From this table we conclude the leptons are indeed pointlike down to distances of about 2×10^{-16} cm. Furthermore there is no evidence for a charged electronlike lepton up to a mass of 40 - 50 GeV.

II.2 ELECTROWEAK EFFECTS

The interference between the electromagnetic and the neutral weak current[20] will change the normalized QED cross section for muon and tau pair production by ΔR and lead to a forward backward asymmetry A in the angular distribution of the leptons in the final state. At present PETRA and PEP energies these effects can be written[21] as:

$$\Delta R = \left(\frac{G_F}{2\cdot\sqrt{2}\cdot\pi\alpha}\right)\frac{2s\cdot g_V^2}{(s/m_z^2-1)} + \left(\frac{G_F}{2\cdot\sqrt{2}\cdot\pi\alpha}\right)^2\frac{s^2(g_V^2+g_A^2)^2}{(s/m_z^2-1)^2} \qquad (4)$$

$$A_{\mu\mu} = \frac{F-B}{F+B} = \frac{3}{4}\,\frac{G_F}{\sqrt{2}\cdot\pi\cdot\alpha}\,\frac{s\cdot m_z^2}{s-m_z^2}\,g_A^2 \approx 2.7\cdot 10^{-4}\,\frac{m_z^2\cdot s}{s-m_z^2}\,g_A^2 \qquad (5)$$

Here F and B denotes the number of negative muons (taus) in the forward, respectively in the backward hemisphere. In the standard model[20] with $\sin^2\theta_W = 0.23$, $m_z = 89$ GeV, $g_V = -1/2(1-4\sin^2\theta_W) = -0.04$ and $g_A = -1/2$ where g_V and g_A denote the vector and the axial vector coupling of the neutral current to a pair of charged leptons. At $s = 1000$ GeV^2 this leads to $\Delta R = 0.002$ and $A_{\mu\mu} = -0.076$.

The change in ΔR cannot be observed at present energies whereas a measurement of the asymmetry is within reach.

The asymmetry data obtained by the various PETRA groups are listed in Table 2.

Table 2 - Forward-Backward asymmetry in $e^+e^- \to \mu^+\mu^-$

Group	JADE	MARK J	PLUTO	TASSO
$A_{\mu\mu}$(%)	-8 ± 9	0 ± 9	7 ± 10	1 ± 12

The systematic uncertainties are quite small and the data from the various groups can therefore be combined. The combined angular distribution is plotted in Fig. 6 and it yields $\langle A_{\mu\mu} \rangle = -(0.9 \pm 4.9)\%$ to be compared to the predicted value of -6% including acceptance corrections.

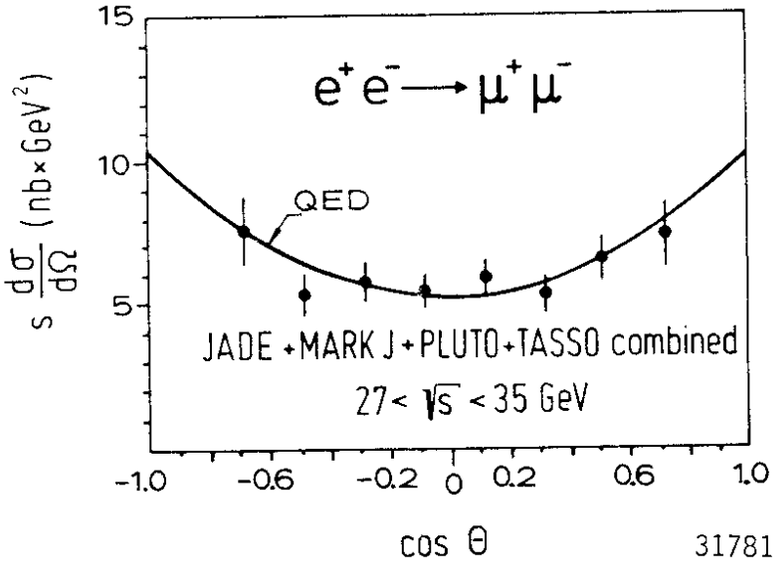

Fig. 6

The combined angular distribution of $s\, d\sigma/d\Omega$ for $e^+e^- \to \mu^+\mu^-$ at c.m. energies between 27 and 35 GeV.

The 95% upper confidence limit is $|A_{\mu\mu}| < 9\%$ i.e. $g_A^e \cdot g_A^\mu < 0.375$ compared to the theoretical value of 0.25 in the standard model.

The relative deviation of the Bhabha cross section due to weak effects, is plotted[22] in Fig. 7 versus scattering angle for various values of m_z. Also indicated are the deviations expected for a cut off parameter Λ of 250 GeV. It is clear that weak effects in $e^+e^- \to e^+e^-$ cannot be parametrized in terms of Λ and they should be included in the theoretical cross section before extracting a value for Λ.

The deviation of Bhabha scattering from the lowest order QED prediction as measured by MARK J from c.m. energies between 29.9 and 35.8 GeV is plotted in Fig. 8 and compared to various predictions of the standard model with $\sin^2\theta_W = 0.25$, 0.01 and 0.55 respectively. Note that they can only determine the cross section between 0^o and 90^o since they do not determine the charge. The data favours $\sin^2\theta_W = 0.25$ however, better data at higher energies are needed to set stringent limits on $\sin^2\theta_W$ from this reaction.

Using the standard model the data on $e^+e^- \to e^+e^-$, $e^+e^- \to \mu^+\mu^-$ has been used to extract values on $\sin^2\theta_W$. The results are listed in Table 3.

Table 3 - Results on $\sin^2\theta_W$

Group	limits on $\sin^2\theta_W$ lower	upper	$\sin^2\theta_W$
MARK J	0.07	0.42	0.24 ± 0.11
JADE	-	0.55	0.25 ± 0.18
PLUTO	-	0.57	0.23 ± 0.17
TASSO	-	0.52	-

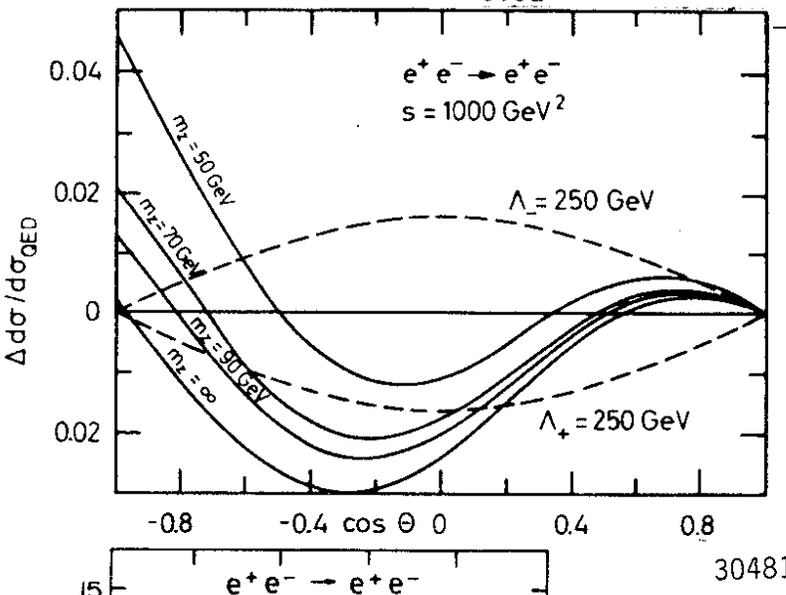

Fig. 7
Relative deviation of Bhabha cross section from the QED prediction plotted versus the scattering angle for various values of m_Z. The dashed curves show the deviations expected for a cut off parameter of 250 GeV.

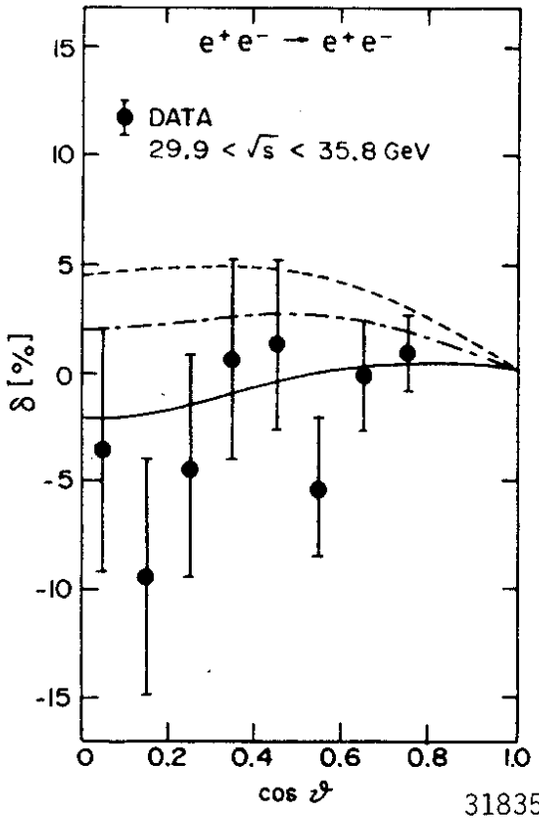

Fig. 8
The difference between the measured cross section for $e^+e^- \to e^+e^-$ and the QED prediction plotted versus the scattering angle θ. Predictions based on the standard model with $\sin^2\theta_W = 0.55$, 0.01 and 0.25 are shown in the dashed, the dashed-dotted and the solid curve respectively. The data are from MARK J.

It is clear that the present data from e^+e^- interactions on neutral currents do not yet compete with the values obtained in neutrino interactions. However, they are the only data which test the theory at high values of Q^2 and they are also the only data which yield information on the neutral weak coupling to muons and taus.

It is possible[23] to construct gauge models which reproduce the low energy data but have a richer spectrum of vector bosons. In such models $g^2_V = 1/4\ (1-4\ \sin^2\theta_W)^2 + 4\ C$ and $g_V\ g_A$ and g^2_A remain unchanged.

JADE and MARK J have determined[2,24,25] the limits on C from measurements of Bhabha scattering and muon pair production. They find with 95% confidence:

JADE	-0.059	<	C	<	0.033
MARK J	-0.097	<	C	<	0.027 .

There are various ways to realize such models. For example SU(2) x U(1) x U'(1)[26] will have only one charged but two neutral vector bosons. In this case

$$C = \cos^4\theta_W\ (m_z^2/m_1^2 - 1)\ (1 - m_z^2/m_2^2) \qquad (6)$$

here m_z is the mass of the Z^0 in SU(2) x U(1) and m_1 and m_2 are the masses of two neutral bosons in the extended model.

It is also possible to construct a model with SU(2) x SU'(2) x U(1)[27]. Such a model will have two charged and two neutral vector bosons, and in this case the $\cos^4\theta_W$ factor is replaced by $\sin^4\theta_W$.

The limit on C can therefore be translated into limits on m_1 and m_2 using the expressions given above. The results are plotted in Fig. 9.

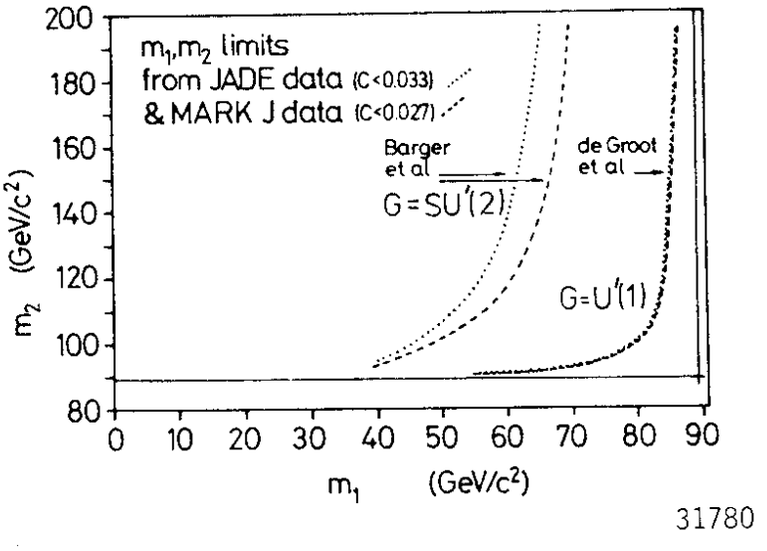

Fig. 9 - Limits on the mass of neutral vector bosons.

II.3 HEAVY LEPTONS

It seems reasonable to expect that the charged lepton in a new generation of elementary fermions is lighter than the quarks. Leptons are pairproduced with a known cross section and decay either leptonically $L \to \ell \bar{\nu}_\ell \nu_L$ or semileptonically $L \to \nu_L$ hadrons. All the groups working at PETRA have searched[2,28] for new leptons. No evidence was found, and the limits set on the mass of a new lepton are summarized in Table4.

Table 4 - Mass limits on new leptons

Group	PLUTO	MARK J	TASSO	JADE
	14.5	16.0	15.5	17

PLUTO and MARK J have searched by selecting events in which a single high energy muon was recoiling against many hadrons. PLUTO demanded that the visible energy of the event should be greater than 3.0GeV and the missing momentum greater than 2.5 GeV/c. Furthermore the thrust should be less than 0.95. MARK J required that the visible energy should be greater than 10% but less than 50% of the c.m.energy. The acoplanarity should be greater than 30^0. The acoplanarity is defined as the absolute value of $(180^0 - \delta\phi)$, where $\delta\phi$ is the angle between the muon momentum vector and the total energy flow vector (see below) of the hadrons $\vec{E}_H$ projected on a plane perpendicular to the beam line. The energy deposited in the outer calorimeter should be $0.1\ E_{vis}$. The event should contain more than two charged tracks and the polar angle between the beam line and the energy flow vector should be between 30^0 and 150^0.

TASSO selected events in which a single isolated charged particle with momentum greater than 1.5 GeV/c was separated by at least 90^0 from any other charged track. The event should contain at least 5 charged tracks and the charged energy should be greater than 8.0 GeV (9.3 GeV) at 30 GeV (35 GeV) in c.m. A similar search was also made requiring the track to be a lepton.

JADE considered events with a visible energy between 11 GeV and 32 GeV produced at 35 GeV in c.m. They searched for non coplanar events as follows: They defined two planes, the first plane was defined by the thrust of one of the "jets" and the e^+ direction, the second plane by the momentum of the remaining particles. The opening angle between the two planes should be greater than 45^0, and the angle between the thrust axis and the e^+ direction should be at least 45^0.

In the present phenemenology[29] of supersymmetric[30] theories all particles will have partners which differ in spin by half a unit. Thus there will be scalar electrons (muons) which can be pairproduced in e^+e^- annihilation and which may decay into electrons (muons) and undetectable particles (photinos, goldstinos) leading to acoplanar two prong electron (muon) events. No evidence[2,28] was found resulting in the following limits on the mass of a scalar lepton: PLUTO $m_s >$ 13 GeV, JADE $m_s > 16$ GeV, MARK J $m_s > 16$ GeV.

III. HADRON PRODUCTION IN e^+e^- ANNIHILATION

It has been conjectured[31-34] in the naive parton model that hadron production in e^+e^- annihilation proceeds by quark-antiquark pair production as shown in Fig.10a, where the electromagnetic current couples proportional to the charge of a pointlike quark. The neutral weak current is expected to contribute on the order of 1% to the total cross section at $s = 1000\ GeV^2$ energies and is neglected. The total cross section for hadron production in this approximation should therefore be proportional to the cross section for muon pair production with the constant of proportionality

$$R = \frac{\sigma(e^+e^- \to \text{hadrons})}{\sigma(e^+e^- \to \mu^+\mu^-)} = 3 \sum_i \left(\frac{e_i}{e}\right)^2 \qquad (7)$$

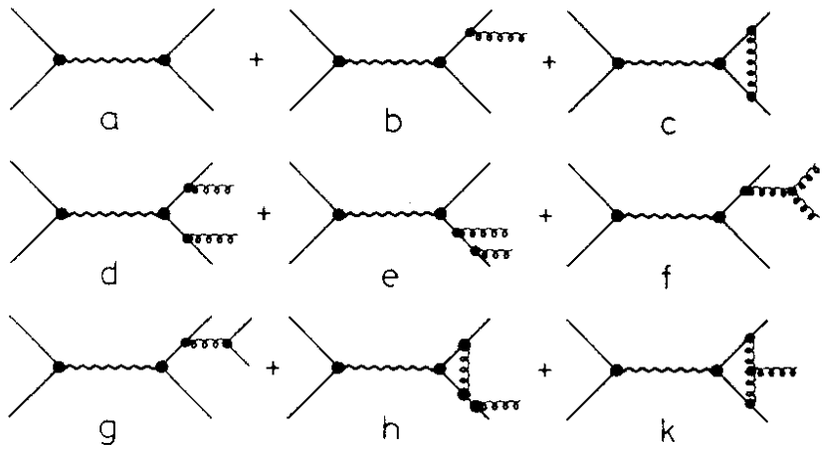

Fig. 10
Some of the diagrams for hadron production in e^+e^- annihilation up to second order in α_s.

Here e_i is the charge of the ith flavour and the sum is over all flavours with masses $< E_{beam}$. The hadrons should then appear in two nearly collinear jets of hadrons with small and maybe constant momenta transverse and large and growing momenta parallel to the jet axis. The single particle distribution should scale i.e.

$$s \cdot \frac{d\sigma}{dx}$$

with $x = E_h/E_{beam}$ should become independent of energy at large energies. The charged particle multiplicity would be expected to increase logarithmically with $s = (2E)^2$. The data[35] from SPEAR and DORIS at lower energies support the gross features of this picture.

This naive parton picture will be modified in any field theory[36] of strong interactions. In a field theory e^+e^- annihilation proceeds to lowest order by the Feynman graphs shown in Fig. 10 b, c. The produced quark radiate field quanta (gluons) and the gluons are expected to materialize as hadron jets in the final state.

This has well defined experimental implications[36-38]: The mean transverse momentum of the hadrons with respect to the jet axis will increase with energy. If the quark-gluon coupling constant is small only one of the two original jets will broaden. A primordial $q\bar{q}g$

state is necessarily planar and the final hadron configuration should retain the planarity. In a small fraction of the events the gluon may be radiated at an angle which is large compared to the angular spread of the hadron jet. Such events will be very striking with three visible jets of hadrons defining a plane. Higher order multiple gluon emission diagrams (Fig. 10d-f)are expected to become more visible at high energies since the angular spread of the hadrons resulting from the non-perturbative fragmentation of a single quark or gluon decreases rapidly with energy, enabling one to pick out at higher energies jets from gluons radiated at smaller angles relative to the primordial q and $\bar{q}$ directions. Such multijet events are of course not planar in general and will lead to an increase of the momentum transverse to the event plane. A field theory of the strong interactions will also modify the value for R given above, the multiplicity will grow faster than ln s and the single particle distribution will no longer scale[36].

At present quantum chromodynamics (QCD)[39] is the leading candidate for a theory of strong interactions. The coupling strength in this theory depends on a characteristic strong interaction mass Λ and a typical momentum transfer q in the process. The functional form is given by:

$$\alpha_s(q^2) = g^2/4\pi = \frac{12\pi}{(33-2N_f)\ \ln\ q^2/\Lambda^2} \qquad (8)$$

where N_f is the number of flavours with mass below threshold.

Although the exact value of Λ is still a subject of some controversy[40] it is presumably rather small, on the order of one to a few hundred MeV.

Here I will first discuss the gross properties of the final state, then summarize the evidence for gluon bremsstrahlung and finally discuss the properties of the gluon in some detail.

IV GENERAL PROPERTIES OF THE FINAL STATE IN e^+e^- → HADRONS

The basic diagrams (Fig. 10) governing e^+e^- → qq(g) → hadrons are very simple. The properties of the hadrons in the final state can therefore be directly related to the properties of quarks and gluons and their fragmentation into hadrons.

IV.1 THRUST AND SPHERICITY DISTRIBUTIONS

The energy dependences of the average sphericity[33] <S> and (1 - <T>), where <T> is the average thrust[41], are plotted versus c.m. energy together with data obtained at lower energies in Figs. 11 and 12.

Both quantities decrease with increasing energies as expected if the jets become more collimated with increasing energies. The jet cone half opening angle, as indicated from the sphericity distribution, shrinks from about 31° at 4 GeV in c.m. to 17° near 36 GeV. However, this decrease is slower than that expected in a pure e^+e^- → $q\bar{q}$ model. The observed decrease is in agreement with computations including gluon bremsstrahlung. Note that the distributions are smooth indicating the absence of thresholds in the

energy range above the $b\bar{b}$ threshold.

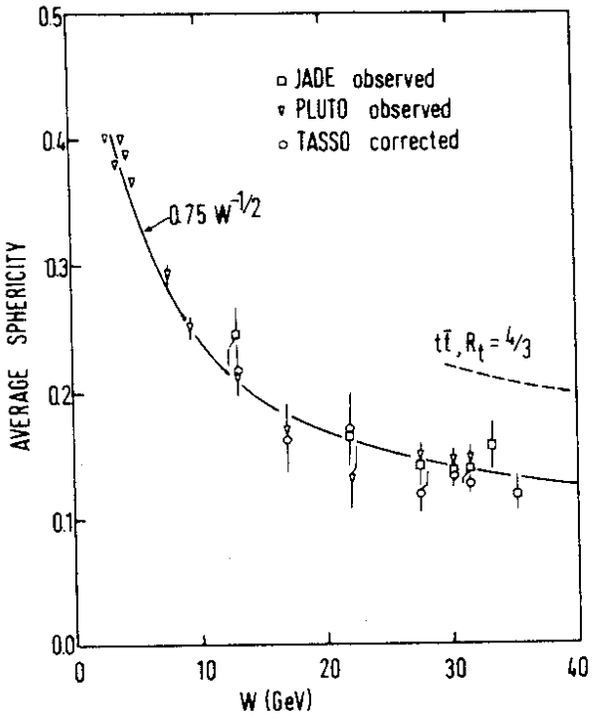

Fig. 11

The average sphericity plotted as a function of c.m. energy.

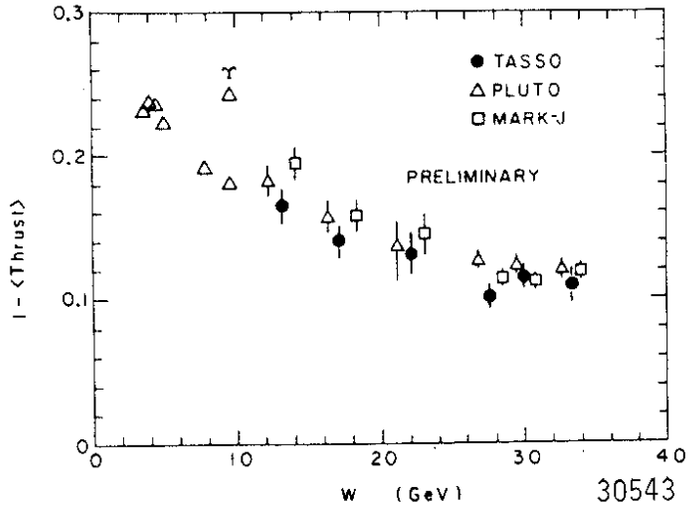

Fig. 12

The average of $1 - \langle T \rangle$ plotted as a function of c.m. energy.

IV.2 THE TOTAL CROSS SECTION

The PETRA groups report[2] data on R for center of mass energies between 12 GeV and 36.5 GeV. The data, corrected for radiative effects including the vacuum polarization and with the contribution from τ pair production removed, are plotted versus c.m. energy in Fig. 13a together with data obtained at lower energies[42].

In the parton model with u, d, s, c and b quarks $R = 3\Sigma_i e_i^2 = 11/3$. This expression is modified[43] in first order QCD to

$$R = 3 \sum_i e_i^2 (1 + \alpha_s/\pi). \qquad (9)$$

At $s = 1000\ GeV^2$, α_s/π is of the order of 5% yielding $R \simeq 3.9$, Higher order terms[43] depend on the renormalization scheme used but they are smaller than the first order term. The QCD prediction, plotted in Fig. 13a, is in agreement with the data.

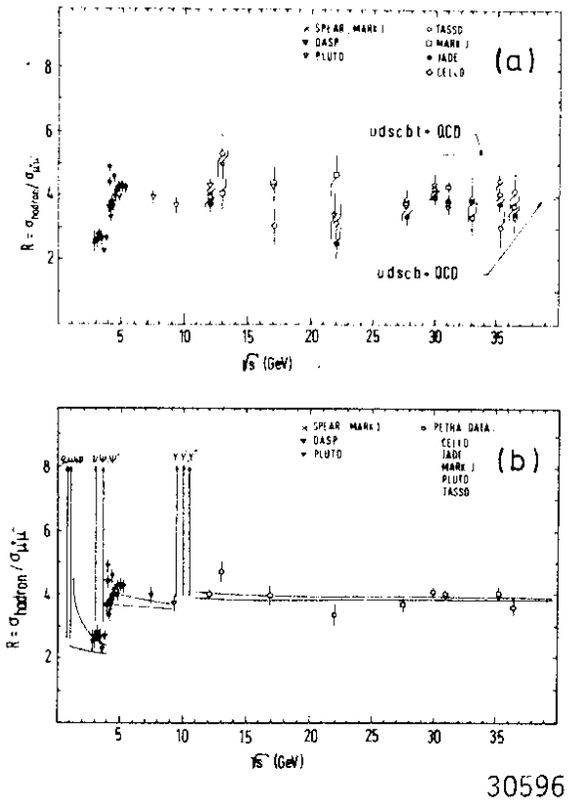

Fig. 13 -
a) The ratio R of the total hadronic cross section normalized to the muon pair cross section is plotted as a function of c.m. energy.
b) The value of R obtained by averaging the data of all the PETRA groups. The solid line represents two QCD predictions with $\Lambda = 1.0$ GeV (upper curve) and $\Lambda = 0.1$ GeV (lower curve).

Are the QCD corrections needed to fit the data ? Clearly not, since the systematic errors are believed to be of the order of 10%. However, note from Fig. 13a that the data which were collected using different trigger conditions and analysed using different cuts are in agreement within the statistical errors. This indicates that the systematic errors may be smaller than 10% and indeed there are good reasons to expect that R can eventually be measured rather well in the PETRA energy range.

It is therefore tempting to add the data from the various groups and the resulting cross section is plotted in Fig.13b. The solid lines are QCD predictions corresponding to $\Lambda = 1.0$ GeV and 0.1 GeV respectively. Averaging all the data above 20 GeV in c.m. yields $R = 3.97 \pm 0.06$. An error of 0.16 was computed from the fluctuations of the individual measurements. First order QCD at $s = 1000\ GeV^2$ predicts $R = 3.87$ for $\Lambda = 100$MeV or $R = 3.94$ for $\Lambda = 500$ MeV.

IV.3 THE NEUTRAL ENERGY FRACTION

The JADE Collaboration has determined[3] the fraction of the total energy converted into photons by a direct measurement of the photon energy deposited in lead glass counters surrounding the detector. They have also determined the total neutral energy fraction by measuring the energy carried away by charged particles and subtracting this from the known c.m. energy. The results, listed in Table 5 show that the neutral energy fraction, which includes K^0_S

and Λ's, increase with energy. Also the energy fraction carried off by photons seems to increase. However, in this case the errors are rather larger.

Table 5 - Energy fraction carried off by photons and by neutral particles

$\sqrt{s}$ (GeV)	Energy fraction carried off by Photons %	Neutral particles %
12	21.3 ± 7.0	31.2 ± 4.1
30.4	26.1 ± 5.9	37.5 ± 3.7
34.9	30.7 ± 6.0	43.8 ± 4.1

IV.4 CHARGED MULTIPLICITIES

The average charged multiplicity $\langle n_{ch} \rangle$ observed at high energies[44-46] is plotted in Fig. 14 together with data obtained at lower

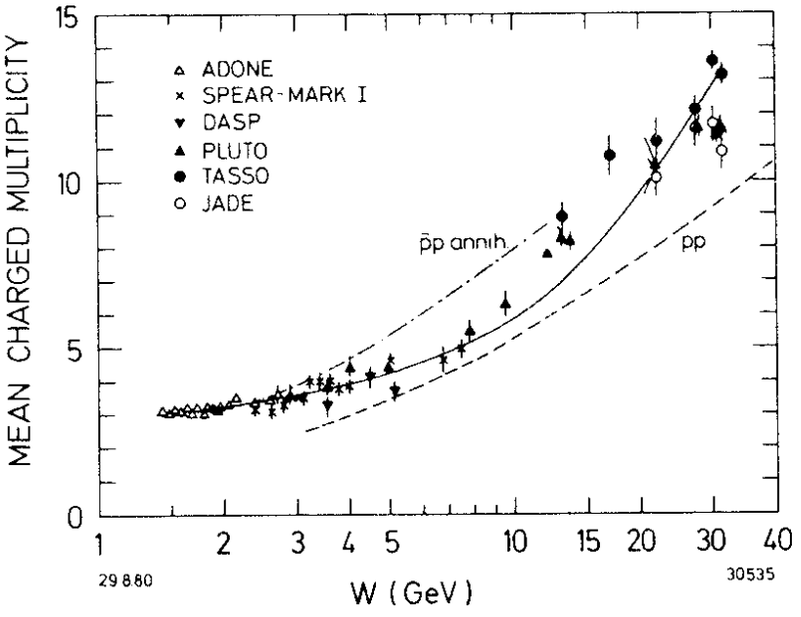

Fig. 14

Average charged particles multiplicity versus the c.m. energy. The solid line is a combined fit to the low energy data and the TASSO data at high energies.

energies[47]. The high energy data points from the various groups are in reasonable agreement and are well above the multiplicities obtained by extrapolating the lower energy data according to a + b ln s as predicted by the naive quark-parton model. For comparison, the multiplicities observed in pp[48] and $\bar{p}p$[49] are also shown.

The average multiplicity in QCD may[50-51] increase as $n = n_o + a \exp(b\sqrt{\ln s/\Lambda^2})$, and the data can indeed be fitted over the whole energy range using this form. The values of the parameters obtained by fitting the TASSO and the PLUTO data are listed in Table 6. The fit considers only the statistical errors and the results were obtained assuming Λ = 0.5 GeV/c.

Table 6. - Fits to the charged particle multiplicity

Group	n_o	a	b
TASSO	2.92 ± 0.04	2.85 ± 0.07	0.0029 ± 0.0005
PLUTO	2.38 ± 0.09	1.92 ± 0.07	0.04 ± 0.01

The asymptotic value[51] of a = 2.4 in QCD. However, note that the fragmentation of the gluon in three jet events is expected to increase the average multiplicity by less than one unit at the highest energy.

IV.5 INCLUSIVE PARTICLE SPECTRA

The scaled cross sections $s\,d\sigma/dx$ for inclusive charged particle production as determined by DASP[47], SLAC-LBL[52] and TASSO[3,53] for c.m. energies between 5 GeV and 36.6 GeV are plotted in Fig. 15 versus x.

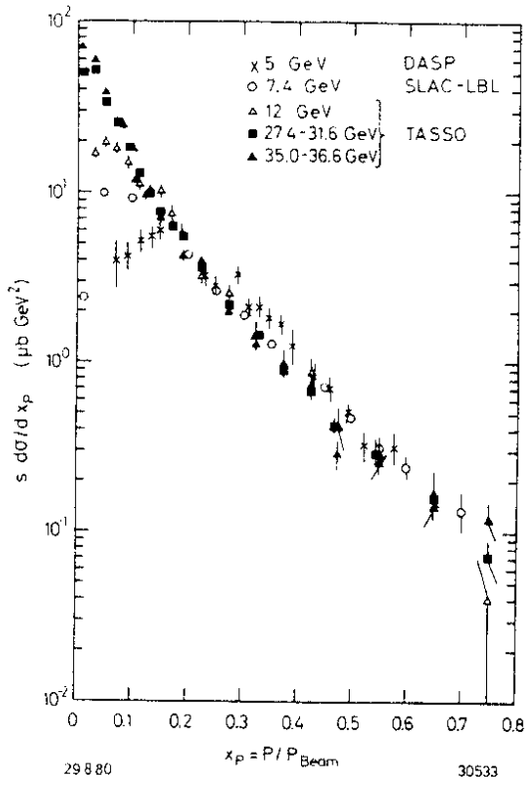

Fig. 15 - The scaled cross section $s\,d\sigma/dx$ ($x = p/p_{beam}$) for inclusive charged particle production.

The cross section for x > 0.2 scales to within 30% between 5GeV and 36.6 GeV. For x < 0.2 the cross section increases dramatically with energy and shows that the observed increase in multiplicity is due to slow particles. Gluon emission will lead[36] to a depletion of particles at large x and a corresponding increase in the yield at small x, since the energy is now shared between the quark and the gluon. In QCD these are rather small effects except at very large or very small x. In general the effects are only of the order of 10-20% at PETRA energies since q^2 is very large compared to Λ^2.

During the past year the PETRA experiments have succeeded in identifying hadrons over a considerable range in momentum. The available data[3] are summarized in Table 7.

Table 7 - Experiments measuring particle separated cross section

Type of particle	Experiment	Technique	Momentum range(GeV/c)	Remark
$\pi^{\pm}$	JADE	dE/dx [3]	< 0.7, 2-7	preliminary
	TASSO	TOF [54]	< 1.1	
		Cerenkov [3]	< 5.0	preliminary
$K^{\pm}$	JADE	dE/dx [3]	< 0.7	preliminary
	TASSO	TOF [54]	< 1.1	
		Cerenkov [3]	< 5.0	preliminary
$K^0, \overline{K^0}$	PLUTO	$K^0_S \to \pi^+\pi^-$ [3]	all p	preliminary
	TASSO	$K^0_S \to \pi^+\pi^-$ [3]	all p	
p, $\bar{p}$	JADE	dE/dx [3]	< 0.9	preliminary
	TASSO	TOF [54]	< 2.2	
		Cerenkov [3]	< 4.0	

The scaled cross section $s/\beta\, d\sigma/dx$ for charged pions is plotted in Fig. 16 versus x. The TASSO and the JADE data[3,54] are in agreement and seem to fall below the DASP 5.2 GeV data[47].

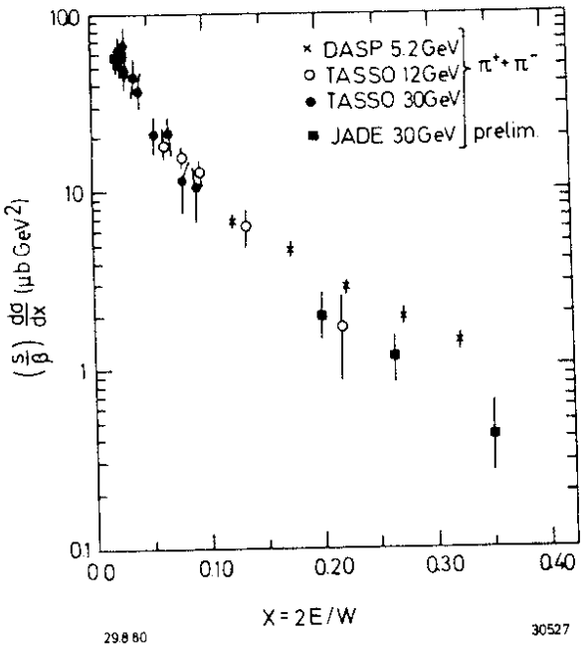

Fig. 16 - The scaled cross section $s/\beta\, d\sigma/dx$ for charged pions.

The data[3,54,55] for neutral and charged kaons measured by TASSO and PLUTO at high energies and by the MARK I Collaboration[56] at lower energies are plotted versus x in Fig. 17. The data are in general agreement, and in particular the cross sections for charged and neutral kaon production are similar. The average value for charged pion production is shown as the solid line. The kaon cross section is a factor of 2 to 4 below the pion cross section at low x but seem to approach the pion data at large x.

The proton data[3,54] are plotted in Fig. 18 and compared to the charged pion data represented by the solid lines. Within the rather large error bars the cross section for kaon and proton production are similar. The large p, $\bar{p}$ cross section seems surprising.

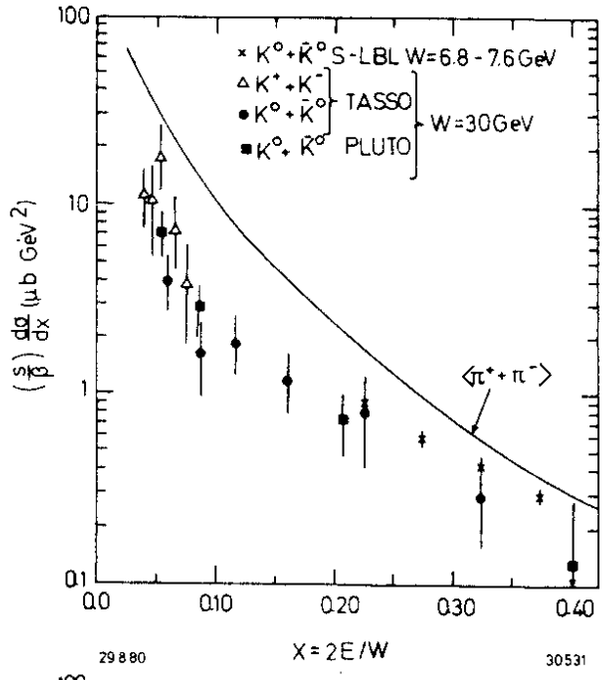

Fig. 17

The scaled cross section $s/\beta\ d\sigma/dx$ for neutral and charged kaons. The average pion cross section is shown as the solid curve.

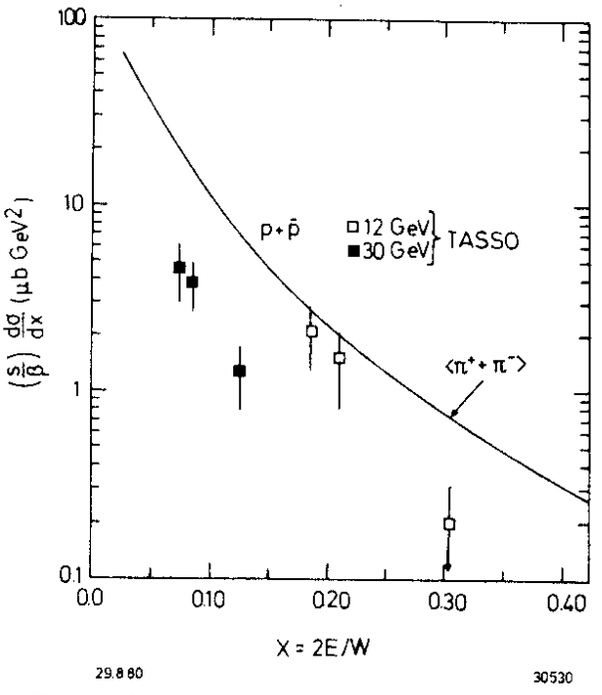

Fig. 18

The scaled cross section $s\beta\ d\sigma/dx$ for protons. The average charged pion cross section is shown as the solid curve.

The relative fractions of charged pions, kaons and protons observed at 30 GeV in c.m. are plotted in Fig. 19 as a function of particle momentum. At low momenta nearly all the particles are pions, however, the kaon and the proton yield rises rapidly with momentum such that at a momentum of 3.0 GeV/c the ratio of

$\pi^{\pm}$ to $K^{\pm}$ to $p^{\pm}$ is roughly 55 to 35 to 10.

An average event at a center of mass energy of 30 GeV consists of roughly 10 $\pi^{\pm}$, 1.4 $K^0\bar{K}^0$, 1.4 K^+K^- and 0.4 $p\bar{p}$ i.e. about one out of 5 events

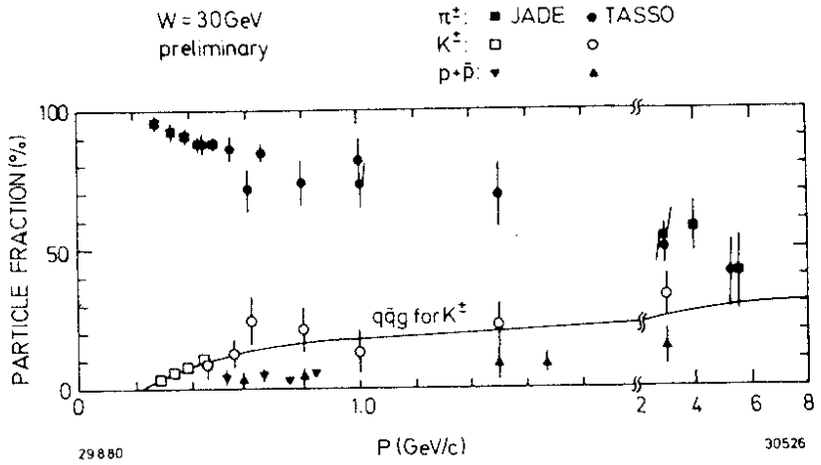

Fig. 19
The relative fraction of charged pions, kaons and protons observed at 30 GeV in c.m.

has an p, $\bar{p}$ pair in the final state.

IV.6 CHARGE CORRELATIONS

The back to back produced quarks have opposite charge. According to the standard picture they will fragment into hadrons by a neutral quark-gluon cascade thus conserving the initial charge. Therefore, apart from fluctuations, the charge found in one jet should be correlated with the charge of the other jet. Furthermore one expects[57] this long range correlation to be found among the fast particles and that the slow particles should exhibit short range correlation only. The TASSO group reports[4] the first evidence for long range correlation.

To investigate the charge correlations they evaluate the function

$$\bar{\phi}(y,y') = -\frac{1}{\Delta y \Delta y'} \langle 1/n \sum_{k=1}^{n} \sum_{i \neq k} e_i(y)\, e_k(y') \rangle \qquad (10)$$

In this expression $e_i(y)$ is the charge of a particle i at rapidity y in the interval Δy and $e_k(y')$ is the charge of a particle k at a rapidity y' in the interval $\Delta y'$. The rapidity is defined as

$$y = \frac{1}{2} \ln \left(\frac{(E + p_{\parallel})}{(E - p_{\parallel})} \right) \qquad (11)$$

where $p_{\parallel}$ is the particle momentum along the jet axis. The function $\bar{\phi}(y,y')$ is related to the probability that the particles i and k have opposite sign charges minus the probability that the charges have the same sign. Since the event as a whole is neutral the function $\bar{\phi}(y,y')$ simply shows how the charge of particle i at a rapidity y is being compensated. The normalization is choosen such that $\iint \bar{\phi}(y,y')dy'dy=1$. In Fig.20 the ratio $\phi(y,y') = \bar{\phi}(y,y')/\int \bar{\phi}(y,y')dy$ is plotted versus y with the test particle in the rapidity interval $-0.75 \leq y' \leq 0$, i.e. a slow particle. This distribution peaks at small negative values of y and shows that the charge of a slow particle is indeed compensated locally as expected if only short range correlations are present. The observed peak has an rms width of 1.3.

In Fig. 20 the same quantity is plotted as a function of y for the test particle at $-5 \leq y' \leq -2.5$. Although the bulk of the charge is compensated locally there is now a significant signal at the opposite end of the rapidity plot. Integrating the distribution for $y > 2.5$

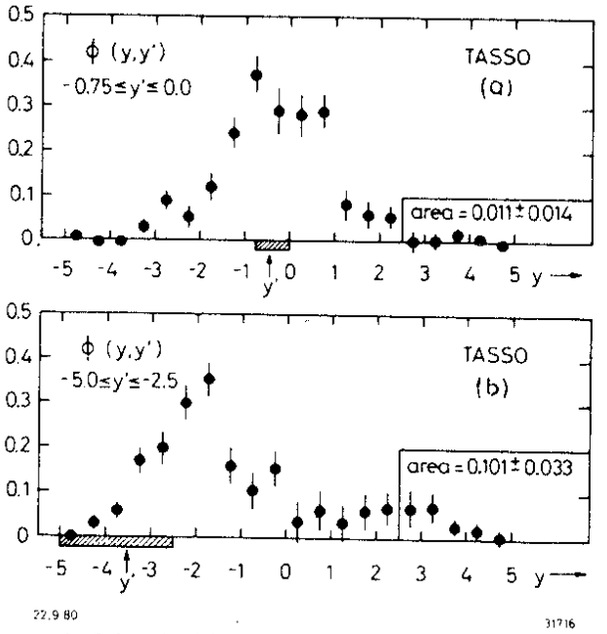

Fig. 20

The charge compensation function $\phi(y, y')$ with the test particle

a) at $-0.75 \leq y' \leq 0$ and

b) at $-5.0 \leq y' \leq -2.5$.

yields 0.101 ± 0.033 compared to the 0.011 ± 0.014 found for the test particle at $-0.75 \leq y' \leq 0$. There is therefore a clear signature for a long range correlation extending over some 7 units in rapidity.

It is interesting to compare the charge correlation to the particle density distribution defined by:

$$\bar{\rho}(y,y') = \frac{1}{\Delta y \Delta y'} < \frac{1}{n(n-1)} \sum_{k=1}^{n} \sum_{i \neq k} |e_i(y)||e_k(y')| > \qquad (12)$$

The quantity $\rho(y,y') = \bar{\rho}(y,y') / \int dy \bar{\rho}(y,y')$ with $\int dy \int dy' \bar{\rho}(y,y') = 1$ is the probability to find a charged particle with rapidity y if there is another charged particle with rapidity y'. This particle density function is plotted in Fig. 21a and b for the test particle at $-0.75 \leq y' \leq 0$ and at $-5 \leq y' \leq -2.5$. Comparing Figs. 20 and 21 shows that the particle density function is wider than the charge correlation function - i.e. unlike sign particles are on the average closer in rapidity than like sign particles.

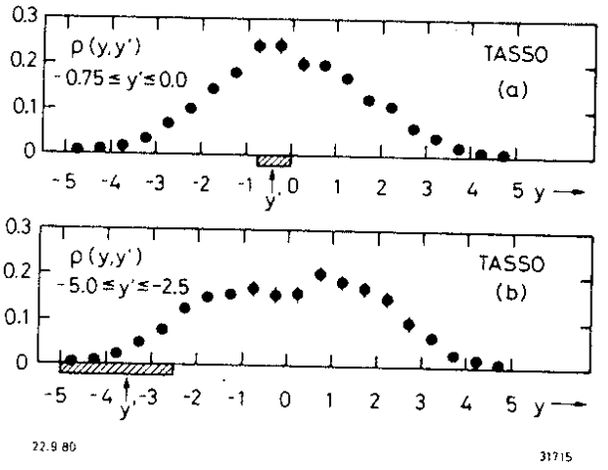

Fig. 21
The particle density function with the test particle

a) at $-0.75 \leq y' \leq 0$ and

b) at $-5.0 \leq y' \leq -2.5$.

The particle density function with the test particles at $-5 \leq y' \leq -2.5$ is rather smooth with no sign of long range correlations.

The correlation functions contain information on the primordial quarks and are more sensitive tests of the fragmentation process than the single particle distributions.

V. EVENT TOPOLOGY AND THE FINAL STATE ANALYSIS

The topology of the hadrons in e^+e^- annihilation can be used to identify the production mechanism

a) Pair production of light quarks with only collinear gluon bremsstrahlung will manifest itself as two collinear jets of hadrons.

b) Single wide angle gluon bremsstrahlung $e^+e^- \rightarrow q\bar{q}g$ leads to planar events with large and growing momenta in the plane and small and limited momenta transverse to the plane. Multiple gluon bremsstrahlung will lead to more isotropic events.

c) Pair production of heavy quarks will yield nearly spherical events close to threshold.

In the next paragraphs we briefly describe the ingredients used in the Monte Carlo simulations and the methods used to determine the topology of the hadrons in the final state.

V.1 INPUTS TO THE MONTE CARLO SIMULATION

All groups have made extensive Monte Carlo computations to confront the various production mechanismns with the data. The inputs to these calculation are summarized below:

a) Quark pairs are pair-produced proportional to e_i^2. Light quark pairs are created from the vacuum in the ratio $u\bar{u} : d\bar{d} : s\bar{s} = 2 : 2 : 1$.

b) The basic gluon bremsstrahlung process (Fig. 10) is treated to first order in the strong coupling constant α_s by Hoyer et al.[58] whereas the computation by Ali et al.[59] includes all second order diagrams except those with internal gluon lines (Fig. 10 h, k).

The formalism of Field and Feynman[60] or the one set up by the Lund group[61] is then used to compute the fragmentation of the constituents.

c) The fragmentation of the quarks is described by 3 parameters in the Field-Feynman model:

i) a_F: The quark fragments $q \rightarrow q' + k$ according to a distribution function $f^h(z) = 1 - a_F + 3a_F(1-z)^2$ with $z = (p_{\parallel} + E)_h/(p_{\parallel} + E)_q$. a_F is the same for u, d and s quarks and is determined experimentally. For the heavy quarks c and b; $f^h(z)$ = constant.

ii) σ_q: The primordial transverse momentum distribution of the quarks with respect to the jet axis is given by $\exp(-p_T^2/\sigma_q^2)$.

iii) P/(P+V): Only pseudoscalar (π, K ...) and vector mesons (ρ, K ...) are produced; P/V is the ratio of pseudoscalar to vector mesons produced in the primordial cascade.

Field and Feynman found[60] that deep inelastic lepton-hadron reactions and also hadron-hadron interactions can be simultaneously described by the following values of parameters:

$$a_F = 0.77, \quad \sigma_q = 0.30 \text{ GeV/c and } P/(P+V) = 0.5.$$

d) The fragmentation of gluons is treated as a two-step process in which the gluon first fragments into a $q\bar{q}$ pair which subsequently fragments into hadrons as outlined above. In the Hoyer et al. program[58]

the gluon imparts all its energy to one of the quarks - i.e. in this model quark and gluon fragmentation are identical, Ali et al.[59] describe $g \to q\bar{q}$ by the splitting function[62] $f(z) = z^2 + (1-z)^2$ where $z = E_g/E_q$.

V.2 EVENT TOPOLOGY

The production mechanism can be delineated from the event shape. There are by now several methods used to determine the shape and the topology of an event. These methods are briefly discussed below.

The shape of an event is conveniently evaluated by constructing the second rank tensor[33,35]

$$M_{\alpha\beta} = \sum_{j=1} p_{j\alpha} \cdot p_{j\beta} \quad (\alpha, \beta = x, y, z) \tag{13}$$

where $p_{j\alpha}$ and $p_{j\beta}$ are momentum components along the α and β axes for the j^{th} particle in the event. The sum is over all charged particles in the event. Let $\vec{n}_1$, $\vec{n}_2$, $\vec{n}_3$ be the unit eigenvectors of this tensor associated with the normalized eigenvalues Q_i, where $Q_i = \Sigma(\vec{p}_j \cdot \vec{n}_i)^2 / \Sigma \vec{p}_j^2$. These eigenvalues are ordered such that $Q_1 \leq Q_2 \leq Q_3$ and are normalized with $Q_1 + Q_2 + Q_3 = 1$. The principal jet axis is then the $\vec{n}_3$ direction. The event plane is spanned by $\vec{n}_2$ and $\vec{n}_3$; and $\vec{n}_1$ defines the direction in which the sum of the square of the momentum component is minimized. Every event can be represented in a two dimensional plot of aplanarity $A = (3/2)\, Q_1$ (i.e. normalized momentum squared out of the event plane) versus sphericity $S = (3/2)(Q_1 + Q_2)$. In such a plot two jet events will cluster at small values of A and S, planar events have small values of A whereas both A and S will be large for spherical events. This is borne out by the Monte Carlo results shown in Fig. 22. This method has been used by TASSO[6] and JADE[9].

MARK J[7,63] uses a linear method based on energy flow where the coordinate system is defined as follows: the $\vec{e}_1$ axis coincides with the thrust axis which is defined as the direction of maximum energy flow. They next investigate the energy flow in a plane perpendicular to the thrust axis. The direction of maximum energy flow in that plane defines a direction $\vec{e}_2$ with a normalized energy flow

$$\text{major} = \sum_i |\vec{p}^{\,i} \cdot \vec{e}_2| \,/\, E_{vis} \tag{14}$$

where $E_{vis} = \Sigma|\vec{p}^{\,i}|$. The third axis $\vec{e}_3$ is orthogonal to both the thrust and the major axis $\vec{e}_2$, and it is very close to the minimum of the momentum projection along any axis i.e.

$$\text{minor} = \sum_i |\vec{p}^{\,i} \cdot \vec{e}_3| \,/\, E_{vis}. \tag{15}$$

The PLUTO group[64] has developed a two step cluster method to determine the event topology. The first stage associates all particles into preclusters irrespective of their momenta. Particles belong to the same precluster if the angles between any two tracks are less than a limiting angle α. The momentum of a precluster is the sum of the momenta of all the particles assigned to that precluster. The preclusters are then combined to clusters if the angle between the momentum vectors is less than a given value β. The number of clusters

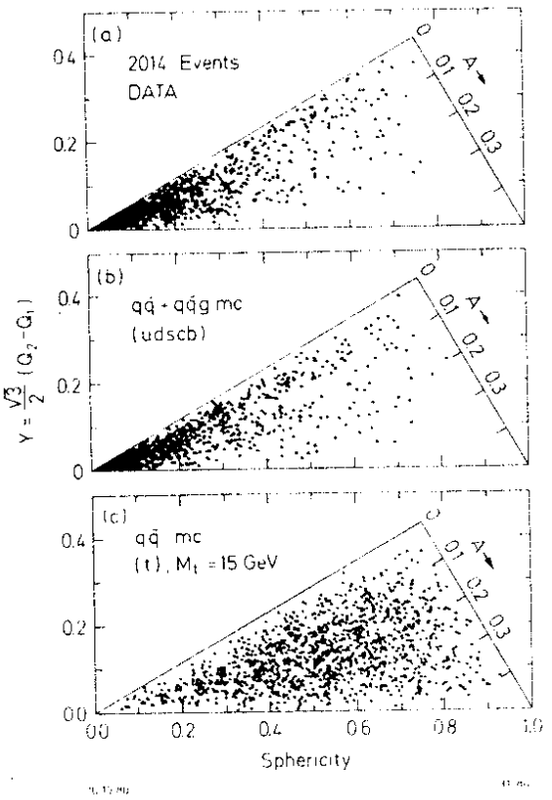

Fig. 22

a) The event distribution in aplanarity and sphericity observed by the TASSO Collaboration between 27.4 GeV and 36.6 GeV in c.m.

Monte Carlo created events in aplanarity and sphericity at 30 GeV in c.m. for

b) $e^+e^- \to q\bar{q}g$ with

$q = u, d, s, c, b.$

c) $e^+e^- \to t\bar{t}$ with

$m_t = 15$ GeV and a c.m. energy of 35 GeV.

n is defined as the minimum number of clusters which fulfil the inequalities;

$$\sum_{i=1}^{n} E_{ci} > E_{vis}\,(1 - \varepsilon) \qquad (16)$$

where E_{ci} is the cluster energy and ε a small number. If the energy of a cluster, defined as the sum of the energies of all particles assigned to the cluster, exceeds a threshold energy E_{th} then the cluster is called a jet. Typical values for the various parameters are $\alpha = 30^0$, $\beta = 45^0$, $\varepsilon = 0.1$ and $E_{th} = 2.0$ GeV.

V.3 EVIDENCE AGAINST NEW QUARKS

The distribution of events in the A, S plane observed[2] by TASSO at c.m. energies between 27.4 and 36.6 GeV is shown in Fig. 22a. The data cluster at small values of S and A with a long tail of planar events as expected for light quark production including gluon bremsstrahlung as shown in Fig. 22b.

In the data at $35.0 \leq W \leq 36.6$ GeV there are 2 events with $A > 0.15$ whereas we expect for a heavy quark a total of 57 events for charge 2/3e and 14 events for a charge 1/3e. Combining these data with similar data[2] from JADE and MARK J excludes a charge 2/3e heavy quark with a mass between the b quark and 18 GeV by some 12 standard deviations. The existence of a charge 1/3e quark is also rather unlikely.

Scanning the cross section has also failed to find any evidence for narrow states. The limit is $\Gamma_{ee} \cdot B_h < 0.4$ keV for c.m. energies between 35.0 and 35.6 GeV. For a charge 2/3e quark or a 1/3e quark we expect to find respectively $\Gamma_{ee} = 5$ keV or 1.3 keV.

VI. GLUONS

At present QCD is the only theory of strong interactions available, and it is obviously crucial to carry out clean experiments which either support or refute this theory. The first step is to demonstrate that field quanta, gluons, indeed do exist. However, this is not sufficient since presumably any field theory of strong interactions contains gluons. To "prove" QCD one must demonstrate that the gluon is a flavour neutral, coloured vector particle with gauge couplings.

VI.1 THE EVIDENCE FOR GLUONS

Gluon bremsstrahlung $e^+e^- \to q\bar{q}g$ (see Fig. 10) has well defined experimental signatures.

A) The average transverse momentum of the hadrons with respect to the jet axis will grow with energy. Normalized transverse momentum distributions, measured by TASSO and evaluated with respect to the sphericity axis are plotted in Fig. 23 versus p_T^2 for different c.m. energies. The observed p_T^2 distribution clearly broadens with energy. In QCD the growth is explained as hard non-collinear gluon emission. Fits based on this mechanism are shown in Fig.23. However, it is also possible to fit the data up to moderate values of p_T^2 by increasing σ_q as a function of c.m. energy.

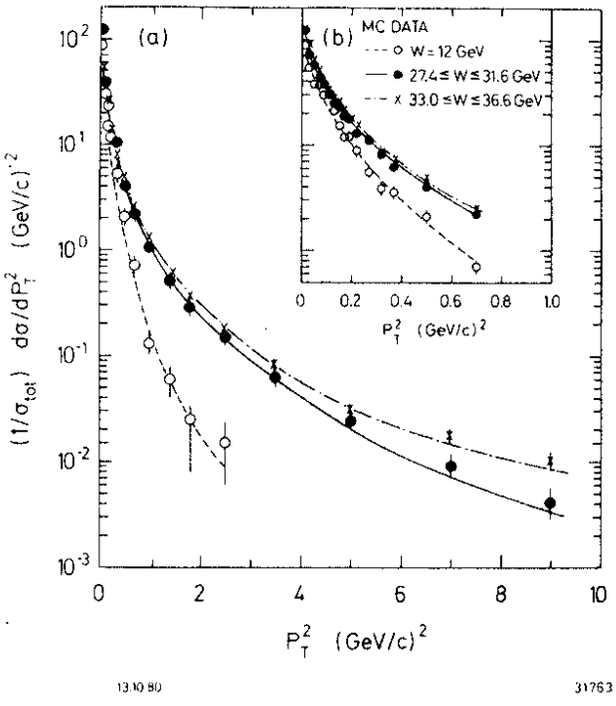

Fig. 23 - $1/\sigma\ d\sigma/dp_T^2$ at 12 GeV, 27.4-31.6 GeV and 33.0-36.6 GeV as a function of p_T^2. The curves are QCD fits to the data with σ_q = 320 MeV/c.

B) If hard non-collinear gluon emission is a rare process as expected in QCD, then there should usually be only one wide-angle gluon per event: In fact the probability of emitting two gluons in one event compared to single gluon emission is proportional to α_s. Hence only one of the jets should broaden.

To test this prediction the jets in an event are divided into a narrow and a wide jet. The data obtained by PLUTO[8] are shown in Fig. 24. Plotted are $\langle p_T^2 \rangle$ versus $z = p/p_{beam}$ at low and high energies for the wide and the narrow jet separately. A large asymmetry between the two jets is observed at high energies. Unlike the asymmetry observed at low energy the PLUTO group find that this cannot be explained by fluctuations in the two jet events.

c) Planarity. Regardless of the value of σ_q (or the mean p_T), hadrons resulting from the fragmentation of a quark must on the average be uniformly distributed

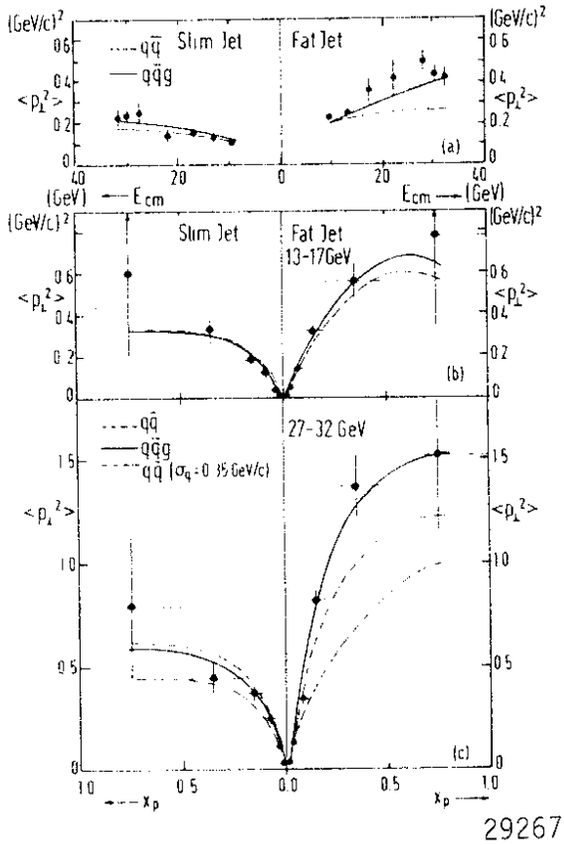

29267

Fig. 24 - Data obtained by PLUTO on $\langle p_T^2 \rangle$ as a function of $z = p/p_{beam}$ for wide and narrow jets. The solid and the dashed curves are the $q\bar{q}g$ and $q\bar{q}$ predictions, respectively.

in azimuthal angle around the quark axis. Therefore, apart from statistical fluctuations, the two jet process $e^+e^- \to q\bar{q}$ will not lead to planar events whereas the radiation of a hard gluon, $e^+e^- \to q\bar{q}g$ will result in an approximately planar configuration of hadrons with large transverse momentum in the plane and small transverse momentum with respect to the plane. Thus the observation of such planar events, at a rate significantly above the rate expected from statistical fluctuations of the $q\bar{q}$ jets, shows in a model independent way that there must be a third confined particle in the final state. The third particle is not a quark since it has baryon number zero and cannot have 1/2 integer spin.

We first compare the distribution of $\langle p_T^2 \rangle_{out}$, the momentum component normal to the event plane squared, with that of $\langle p_T^2 \rangle_{in}$, the momentum component in the event plane perpendicular to the jet axis.

The data obtained by the TASSO group are plotted in Fig. 25 and Fig. 26 for c.m. energies between 12 GeV and 36.6 GeV. The distribution of $\langle p_T^2 \rangle_{out}$ changes little with energy in contrast to the distribution of $\langle p_T^2 \rangle_{in}$ which grows rapidly with energy, in particular there is a long tail of events not observed at lower energies. Fits to the data assuming $e^+e^- \to q\bar{q}$ and σ_q = 300 MeV/c (solid curves) or σ_q = 450 MeV/c (dotted curves) are also shown. The $\langle p_T^2 \rangle_{out}$ distribution at high energies is not fit by σ_q = 300 MeV/c, however by increasing σ_q to 450 MeV/c a good fit can be obtained. The $q\bar{q}$ model however, completely fails to reproduce the long tail observed in $\langle p_T^2 \rangle_{in}$ at high energies. This discrepancy cannot be removed by increasing the mean transverse momentum of the jet. Fig. 25 shows a fit assuming σ_q = 450 MeV/c (which gives a good fit to $1/\sigma\ d\sigma/dp_T^2$ and to $\langle p_T^2 \rangle_{out}$). The agreement is poor. We therefore conclude that the data include a number of planar events not reproduced by the $q\bar{q}$ model independent of the average p_T assumed.

Gluon bremsstrahlung offers a natural mechanism to explain the observed planarity of the events. Fig. 26 shows a second order QCD fit to the data using the Monte Carlo method outlined above. The fit assumed a constant value of σ_q = 320 MeV and α_s = 0.17 (see below). The

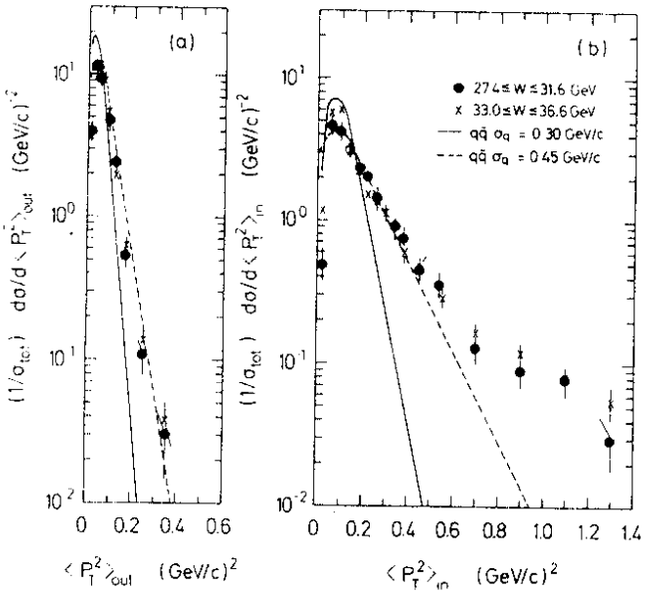

Fig. 25
Distributions of mean transverse momentum squared per event for charged particles, normal to ($\langle p_T^2 \rangle_{out}$) and in ($\langle p_T^2 \rangle_{in}$) the event plane measured by the TASSO Collaboration at low and high energies. The curves are the predictions for a $q\bar{q}$ final state with σ_q = 300 MeV/c (solid lines) and σ_q = 450 MeV/c (dashed lines).

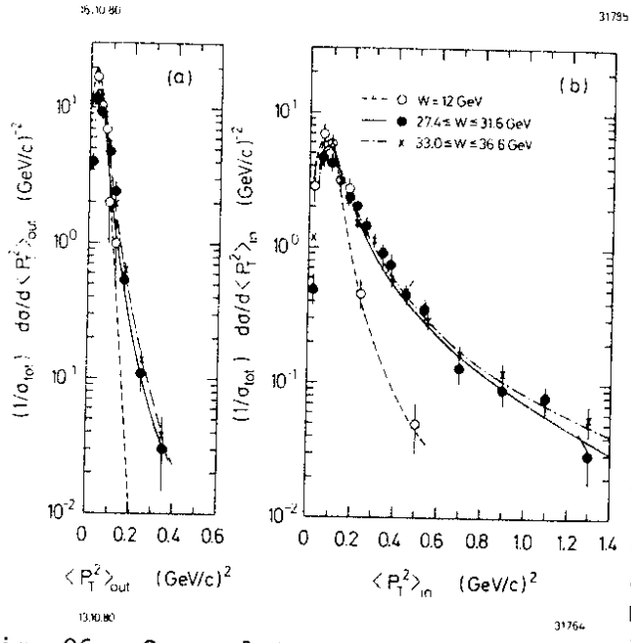

Fig. 26 - Same plot as above. The curves are the second order QCD predictions with α_s = 0.17 and σ_q = 320 MeV/c.

long tail in $\langle p_T^2 \rangle_{in}$ is reproduced in this model. Note that the growth in $\langle p_T^2 \rangle_{out}$ is explained by the occurence at small fraction of 4 (or more) jet events which, in general, are not planar.

The data from PLUTO[8] and JADE[9] analyzed in a similar manner are in full agreement with the findings of the TASSO group.

The planarity of the events is also observed[7,10,63] by the MARK J group using a different technique. They divided each event into two hemispheres using the plane defined by the major and the minor axis (see above) and analyzed the energy distribution in each hemisphere as if it were a single jet. The jet with the smallest transverse momentum with respect to the thrust axis is defined as the narrow jet. the other as the broad jet. The oblateness defined as O = Major - Minor is a measure of the planarity of the event and is zero for phase space and two jet events and finite for three jet final states. The normalized event distribution measured for c.m. energies between 27 and 37 GeV is plotted versus oblateness in Fig. 27 for the narrow and the wide jet separately and compared to the predictions for $e^+e^- \to q\bar{q}$ (dashed curve) and $e^+e^- \to q\bar{q}g$ (solid line). A good fit is obtained with the $q\bar{q}g$ final state whereas the $q\bar{q}$ final state do

not fit the oblateness distribution for the broad jet.

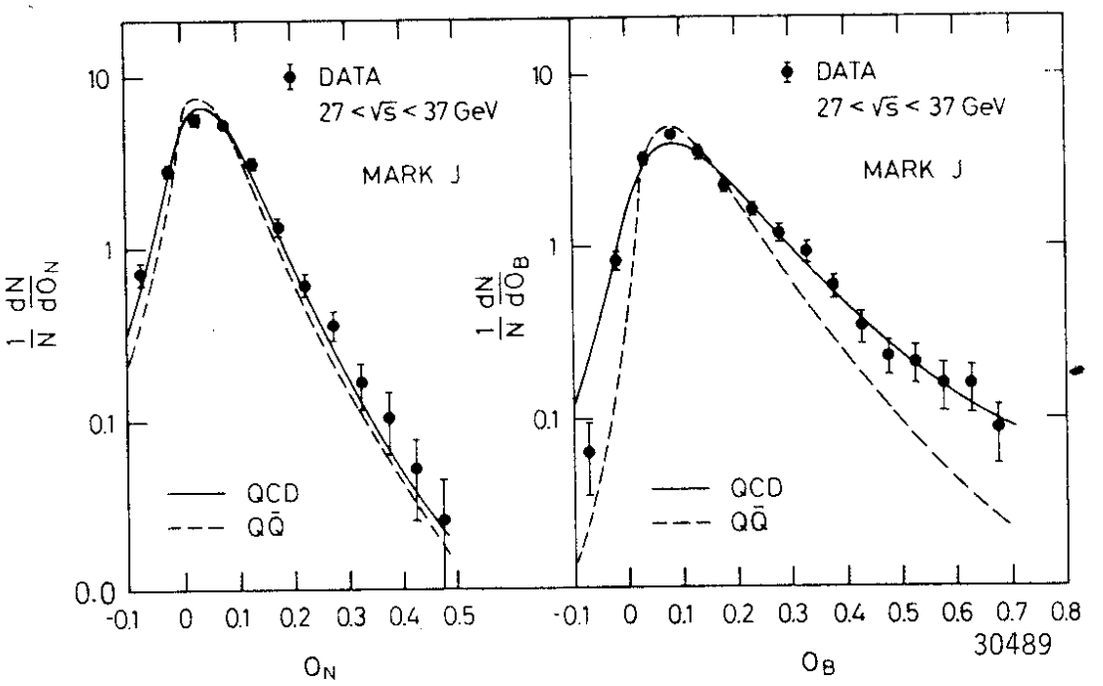

Fig. 27 - The distribution 1/N dN/dO determined by the MARK J Collaboration as a function of oblateness O for the narrow and the wide jet separately. The solid curves are predictions based on $e^+e^- \to q\bar{q}g$, the dashed curve shows the prediction for $e^+e^- \to q\bar{q}$.

The data discussed above prove conclusively that the observed planar events cannot result from the fluctuations in quark pair production with a Gaussian distribution in transverse momentum around the jet axis of the hadrons. Each PETRA group had now observed on the order of 200 planar events with an estimated background from fluctuations of two jet events of about 20%. Wide angle gluon bremsstrahlung $e^+e^- \to q\bar{q}g$ would naturally result in planar events. The observed rate for such events is consistent with the QCD predictions. Besides this source there are two ad hoc possibilities; a flat phase space of unknown origin, or that the transverse momentum distribution of the quark fragmentation has a long non-Gaussian tail. The first possibility can be excluded by observing events with 3 axes, the second by excluding the possibility that the 3 axes are defined by 2 multiparticle jets and a single high momentum particle at a large angle with respect to the jet axes.

D) Properties of planar events. The TASSO Collaboration use a generalization[65] of sphericity to define three-jet events. In this method the tracks are projected on to the event plane defined by $\hat{n}_2$ and $\hat{n}_3$ (see above). The projections are divided into three groups and the sphericity for each group S_1, S_2 and S_3 determined. The three axes and the particle assignment to the three groups are defined by minimizing the sum of S_1, S_2 and S_3. This defines the direction of the three jets and assigns the particles to these jet directions.

In Fig.28 the TASSO events are plotted versus tri-jettiness J_3 defined as

$$J_3 = \langle p_T^2 \rangle_{in} \; / \; (\tfrac{1}{2} (300 \text{ MeV/c}^2)^2).$$

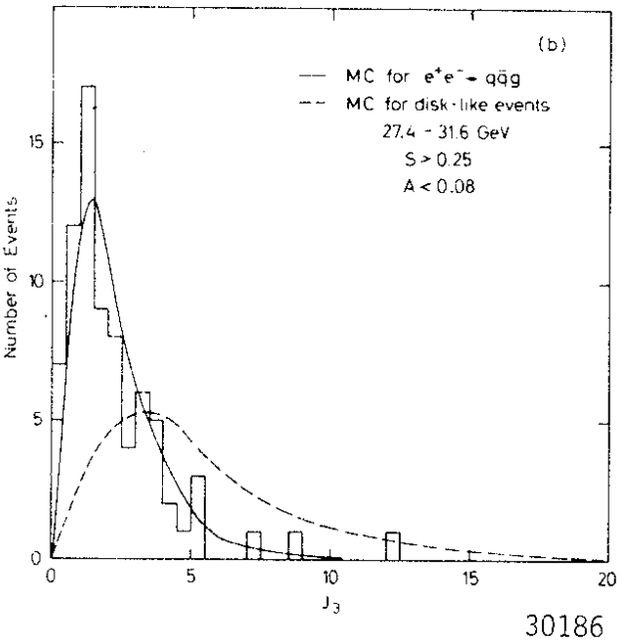

Fig. 28 - Planar events ($S \geq 0.25$, $A < 0.08$) measured by the TASSO Collaboration and plotted versus the tri-jettiness J_3. The Monte Carlo predictions for $e^+e^- \to q\bar{q}g$ (solid) and for $e^+e^- \to$ hadrons (phasespace dashed).

Here $\langle p_T^2 \rangle_{in}$ is evaluated for all charged tracks in an event with respect to their assigned axis. Thus for three jet events with a mean transverse momentum of 300 MeV with respect to the jet axis we expect to find the events clustered around $J_3=1$, compared with a wide distribution in J_3 in case of a flat phase space distribution. The data agree with the expectations for $e^+e^- \to q\bar{q}g$, shown as the solid line. The fit result in χ^2/degree of freedom of 2.3/5. The data disagree strongly with a phase space calculation shown as the dashed line. This fit has a χ^2/degree of freedom of 233/5. Thus the data are not consistent with a phase space distribution.

The TASSO group has also evaluated the transverse momentum of charged particles from three jet events with respect to the jet axes to which they were assigned. This distribution $1/N \; dN/dp_T^2$ is plotted as the solid points in Fig. 29 versus p_T^2. It is compared to the p_T^2 distribution found with respect to the jet axis in two jet events shown as the open points. The agreement is very good and demonstrates that $\langle \sigma_q \rangle$ can be taken to be constant independent of energy, when the events are analyzed as three jet events.

The MARK J group observes a three jet structure in their energy flow analysis. To enhance effects resulting from gluon emission they select events with low thrust $T < 0.8$ and large oblateness $O > 0.1$. Fig. 30 shows the energy distribution of these events in the plane defined by $\vec{e}_1$ and $\vec{e}_2$. Plotted is the energy deposited in 5^0 bins as a function of angle. A clear three peak structure is seen. Plotted are the predictions from QCD, phase space + $q\bar{q}$ with $\sigma_q = 300$ MeV/c and $q\bar{q}$ only with $\sigma_q = 500$ MeV. Normalized to the total event sample, only the gluon bremsstrahlung hypothesis fits the data.

The JADE group[66] uses an independent method suggested by Ellis and Karliner[67] to demonstrate the existence of three jet events. From the data taken at c.m. energies around 30 GeV they select planar events which satisfy the condition $Q_2 - Q_1 > 0.1$ and determine the thrust axis for each event. The event is then divided into two jets by a plane normal to the thrust axis and the p_T for each jet computed separately; the jet with the smallest p_T is called the slim jet, the

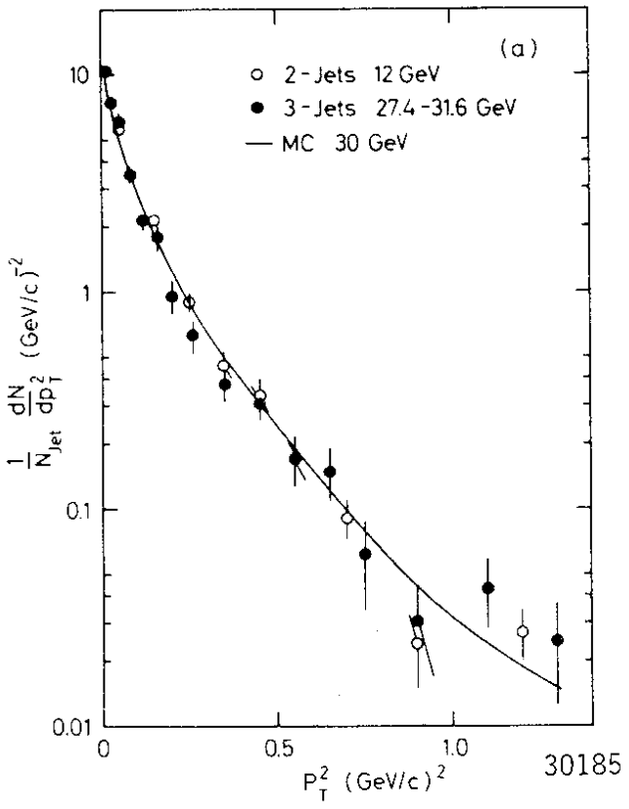

Fig. 29
The transverse momentum distribution $1/N\ dN/dp_T^2$ of the hadrons in the planar events with respect to the three axes found by the generalized sphericity method is shown as the full points. The open points represent the transverse momentum distribution with respect to the jet axis in 2 jet events at lower energies. The solid curve represents the Monte Carlo calculation of $e^+e^- \to q\bar{q}g$ at 30 GeV. The data were obtained by the TASSO group.

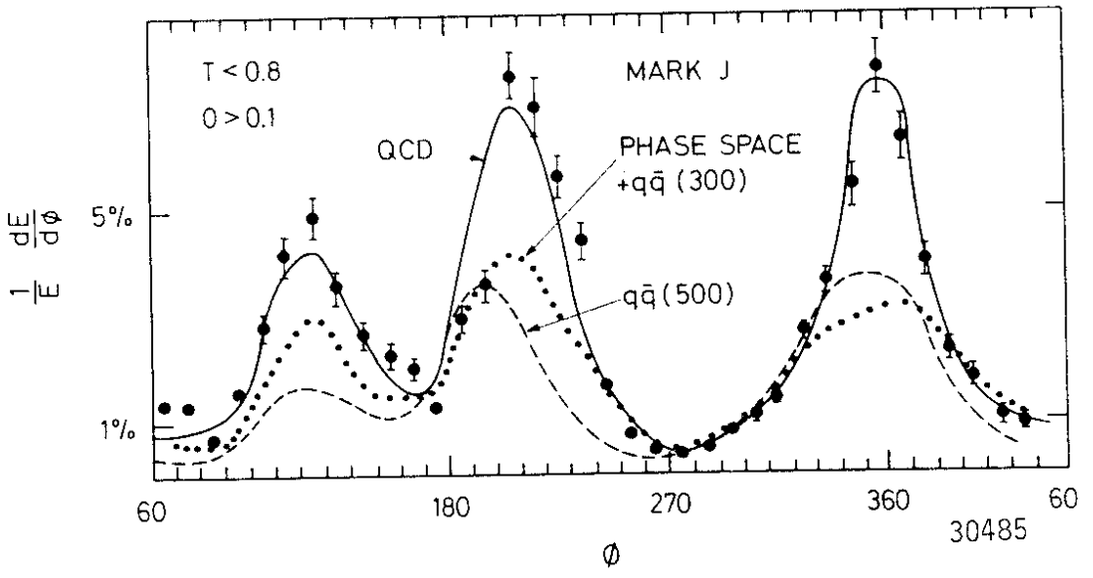

Fig. 30 - A plot of the energy distribution in the plane defined by the thrust and the major axes for all events with thrust < 0.8 and oblateness > 0.1. The measurements were done by the MARK J group. The QCD fit is shown by the solid line, a mixed phase space and $q\bar{q}$ model is shown as the dotted line, a pure $q\bar{q}$ model with σ_q = 500 MeV is given by the dashed line.

other the broad jet. The particles in the broad jet are then transformed into its own rest system. If the broad jet consists of two jets they will now appear as two back to back jets along the new thrust axis T^*. The distribution of T^* in this system is plotted in Fig.31 together with the thrust distribution of two jet events measured at 12 GeV. The two distributions are in excellent agreement. Also other quantities like the invariant mass, mean p_T and charged multiplicity evaluated for the broad jet in its own rest system are in agreement with the same quantities evaluated for a two jet event at 12 GeV. The data therefore exhibit a three jet structure as expected for gluon bremsstrahlung.

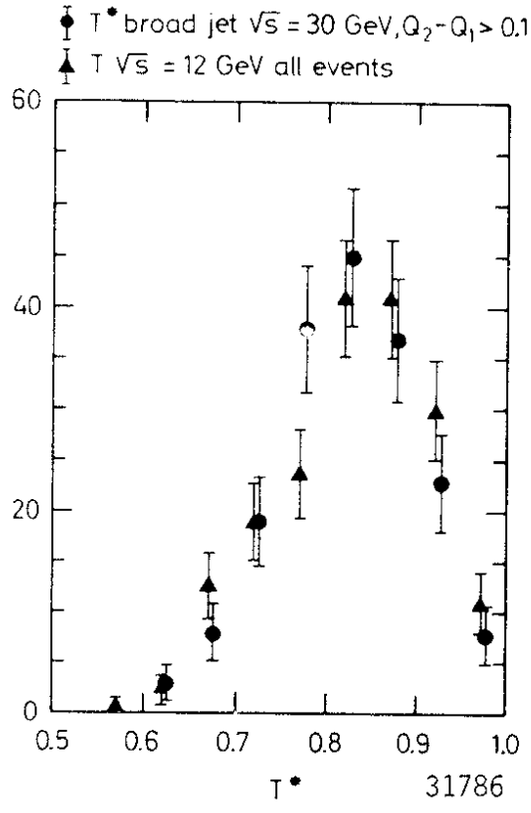

Fig. 31 - Distribution of thrust for the broad jet of planar events at 30 GeV compared with the thrust distribution at 12 GeV. The data were obtained by the JADE Collaboration.

The PLUTO group has analyzed[11,64] their data using the cluster method discribed above. The distribution of the observed number of jets per event are listed in Table 8 and compared to the predictions based on $q\bar{q}$, $q\bar{q}$ + $q\bar{q}g$ (α_s = 0.15) and phase space. The models are all normalized to the number of observed events. The data clearly favour a clustering of the particles around 3 axes.

The remaining question is then to decide whether the third jet is defined by a single particle or a group of particles. This can be done by examining the events. Figs. 32 a and b show typical candidates for three jet events observed by JADE and TASSO. Note that several tracks cluster around each axis.

In Fig. 33 the multiplicity distribution of the three jets determined by the TASSO group is shown. The jets are ordered according to $E_1 > E_2 > E_3$. The energies of the jets were computed from the observed opening angles between the jets neglecting parton masses. Furthermore only events for which the acceptance of the drift chamber is nearly complete were considered. It is clear that each jet in general consists of several charged particles and that the multiplicity distribution is reproduced by the QCD calculation.

In conclusion: all the properties observed in $e^+e^- \rightarrow$ hadrons can be naturally explained by gluon bremsstrahlung. No other alternative mechanism is known which explains all the data. However, to prove that the gluon observed is the QCD gluon we have to show that the gluon is a coloured, flavour neutral vector particle with gauge couplings. There are hints[40] from upsilon decays and from charm and beauty

Table 8 - Number of clusters

n_j	1	2	3	4	5	6	7
Data	2	551	249	53	3	1	
$q\bar{q}$	3	680	152	23	1		
$q\bar{q}+q\bar{q}g$	3	567	247	46	2		
phase space	1	30	154	306	268	86	14

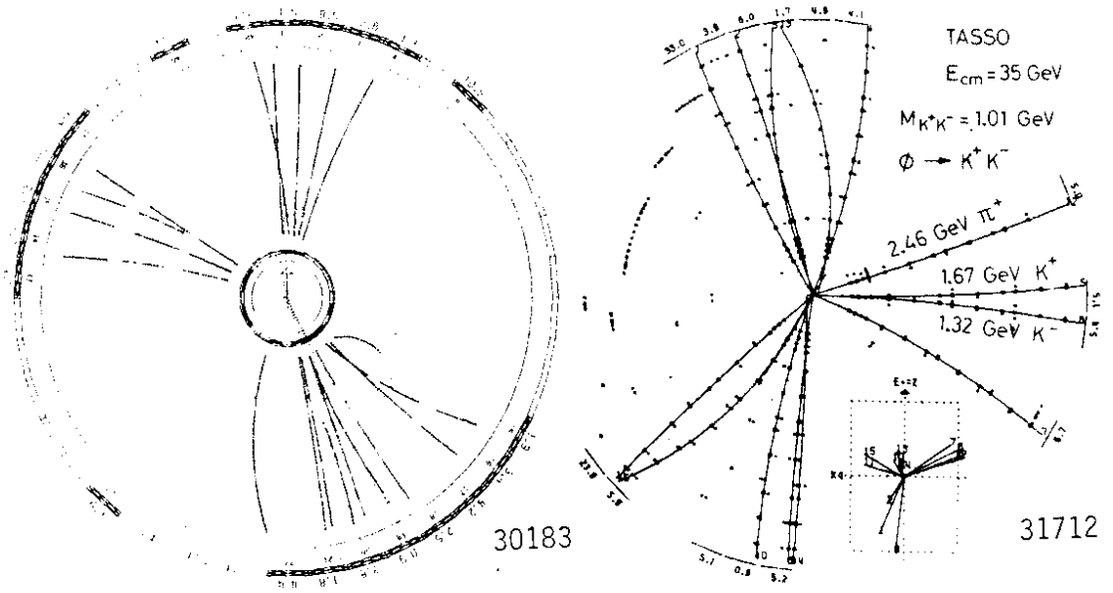

Fig. 32 - Example of three jet events observed by a) JADE and b) TASSO

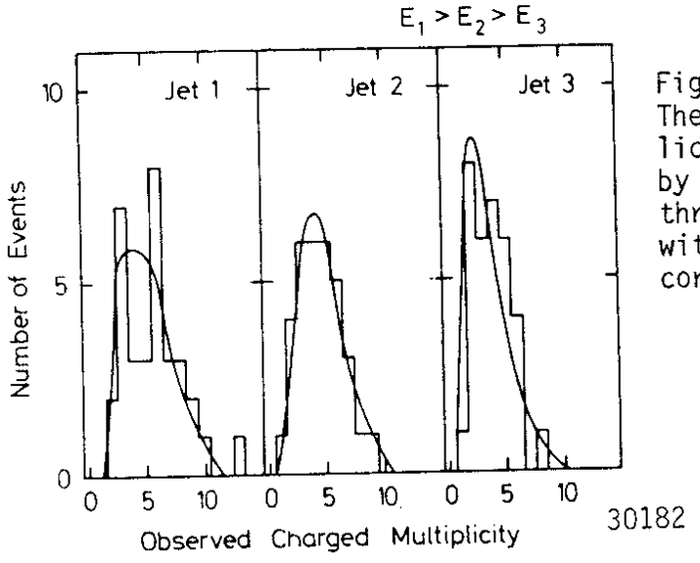

Fig. 33
The charged particle multiplicity distribution observed by TASSO in each of the three jets in a planar event with the jets ordered according to energy.

spectroscopy that the gluon might indeed be coloured and flavour neutral. Determinations of the gluon spin from three jet events will be discussed next.

VI.2 THE SPIN OF THE GLUON

It is obviously crucial to determine the spin of the gluon from a sample of clean three jet events resulting from gluon bremsstrahlung. $e^+e^- \to q\bar{q}g$. This process can conveniently be described in a Dalitz plot using the variables $x_i = E_i/E_b$ where the energy carried off by the quark or the gluon E_i is measured in units of the beam energy E_b. The variables are ordered such that $x_3 < x_2 < x_1$. The thrust of the $q\bar{q}g$ event is then given by x_1, and $x_1 + x_2 + x_3 = 2$.
The distribution of the events as function of x_i, averaged over production angles relative to the incident e^+e^- directions, can be written as

$$\frac{1}{\sigma_0}\left(\frac{d\sigma}{dx_1dx_2}\right)_V = \frac{2\alpha_s}{3\pi}\left(\frac{x_1^2 + x_2^2}{(1-x_1)(1-x_2)} + \text{cyclic permutations of 1,2,3}\right) \quad (17)$$

for the vector case and as

$$\frac{1}{\sigma_0}\left(\frac{d\sigma}{dx_1dx_2}\right)_S = \frac{\tilde{\alpha}_s}{3\pi}\left(\frac{x_3^2}{(1-x_1)(1-x_2)} + \text{cyclic permutations of 1,2,3}\right) \quad (18)$$

for the scalar case.

The TASSO group[68] has determined the spin using the variable $\cos\hat{\theta} = (x_2-x_3)/x_1$ suggested by Ellis and Karliner[67]. $\hat{\theta}$ is the angle between the parton 1 and the axis of the parton 2 and 3 system boosted to its own rest frame. To ensure that the spin analysis is not affected by higher order terms one should avoid x_1 close to 1. Futhermore, for x_1 close to 1 the distributions are varying rapidly so that smearing effects caused by the non-perturbative fragmentation of gluons and quarks are important. For these reasons only events with $1 - x_1 > 0.1$ are used in the analysis.

A total of 248 events remained after this cut, with an estimated two jet event background of 17% and 18% for scalar and vector gluons respectively.

The distribution of the events as a function of $\cos\hat{\theta}$ is plotted in Fig. 34 and compared with the distributions predicted for vector (solid) and scalar (dotted) gluons. The prediction was made using the model of Hoyer at al.[58]. Note that the distributions are normalized to the number of events in the plot i.e. the scalar and vector cases are discriminated using the shape only.

The data clearly favour the vector case. A fit to the data gives for three degrees of freedom $\chi^2 = 1$ for the vector gluon and $\chi^2 = 14.9$ for the scalar gluon - i.e. scalar gluons are disfavoured by 3.1 standard deviations.

One way to avoid binning effects is to evaluate the mean value of the $\hat{\theta}$. The experimental value of $\langle\cos\hat{\theta}\rangle_{exp} = 0.349\pm0.013$ can be compared to the values $\langle\cos\hat{\theta}\rangle_V = 0.341\pm 0.004$ and $\langle\cos\hat{\theta}\rangle_S = 0.298\pm0.003$ for vector and scalar gluons respectively. The experimental value differs from the vector gluon prediction by 0.6 standard deviations and by 3.8 standard deviations for the scalar case.

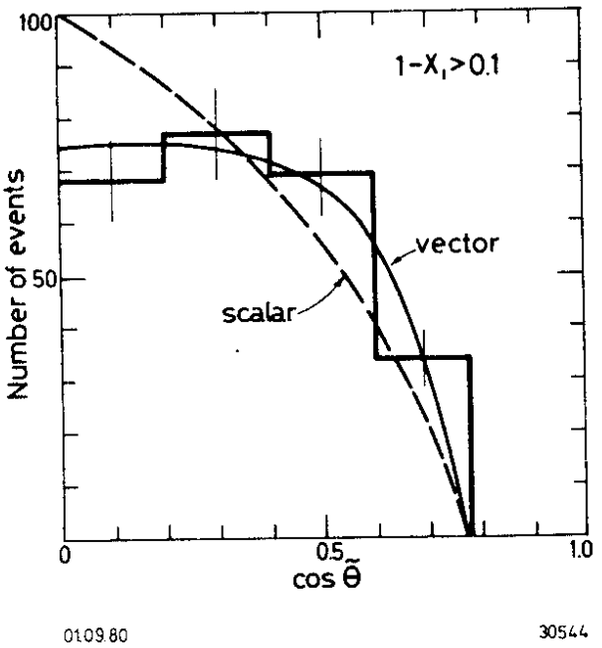

Fig. 34
Observed distribution of the data observed by TASSO in the region $1 - x_1 > 0.10$, as a function of the cosine of the Ellis-Karliner angle $\tilde{\theta}$ defined in Fig. 31b. The solid line shows the QCD prediction and the dotted line the prediction for scalar gluons, both normalized to the number of observed events.

This conclusion is remarkably insensitive both to the exact value of α_s and the details of the fragmentation. Varying the coupling constants by $\pm$ 20% changes the computed value of $\langle\cos\tilde{\theta}\rangle$ by about $\pm$1%. Evaluating $\langle\cos\tilde{\theta}\rangle$ in the elementary model without fragmentation leave the scalar prediction unchanged and increases the predicted value for a vector gluon by about 2%.

Another analysis[11,64] of the gluon spin has been made by the PLUTO Collaboration. They investigate the x_1 distribution - i.e. the distribution of the most energetic jet in three jet events. This distribution is plotted in Fig. 35 with the $q\bar{q}$ contribution subtracted. The prediction for the vector and the scalar case normalized to the number of events is shown as the solid and the dotted curve respectively. The vector curve fits the data nicely whereas the scalar curve is clearly disfavoured. However, note that PLUTO consider events with $(1-x_1) > 0.05$. Removing the last bin would reduce the significance of this fit.

Both the TASSO and the PLUTO conclusions are based on a first order calculation in α_s

VI.3 DETERMINATION OF THE STRONG COUPLING CONSTANT α_s

The strong coupling constant $\alpha_s(s)$ is directly related to the number of three jet events. After choosing a minimum angle between any pair of partons (q, $\bar{q}$ or g) the QCD cross section (Eq.17) can be integrated and normalized to the total e^+e^- annihilation cross section. This ratio depends only on α_s and can be compared directly to the experimental ratio of three jet events to the total number of hadronic events. In practice the analysis must consider several effects:

1) The overlap between jets due to the hadronization process and to fluctuations which might cause a two-jet event to be classified as a three jet event. These effects are not crucial as long as the minimum angle between any two partons is large compared to the opening

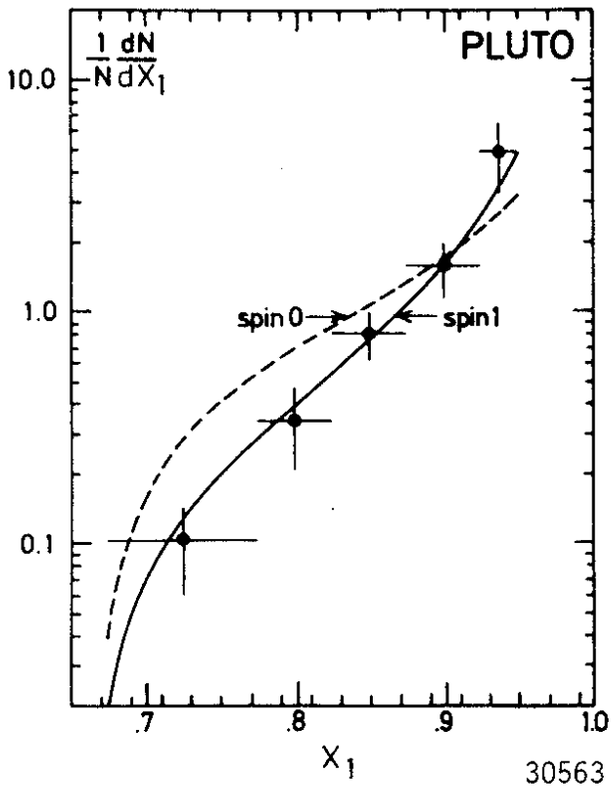

Fig. 35 - The thrust distribution observed by PLUTO in three jet events. The solid line represents the spin 1 case and the spin 0 case is shown by the dotted line. The $q\bar{q}$ contribution has been subtracted.

angle of the jet.
2) The omission of neutrals in some experiments.
3) Apparent multijet contributions resulting from b-decays.
4) Corrections from higher order processes in α_s.
5) QED corrections[68], in particular hard photon emission in the initial state.

These and other effects have been taken into account using the elaborate Monte Carlo routines discussed above.

A first attempt to determine α_s at PETRA energies was made by the MARK J group[69] using data taken around 30GeV. They found, using the Ali et al. program , $\alpha_s = 0.23 \pm 0.02 \pm 0.04$ where ± 0.02 is the statistical error and ± 0.04 the systematic uncertainty. A recent analysis[10] based on further data and which also includes the hard photon correction omitted in the first analysis yields as a preliminary value $\alpha_s = 0.19 + 0.02 + 0.04$.

The TASSO group determined[70] α_s from the event distribution in the A, S plane. They found that α_s can be determined almost independently of the fragmentation parameters using events with $S > 0.25$. In this kinematical region three jet events dominate and non-perturbative effects are not important. The events with $S \geq 0.25$ were fitted for all allowed values of a_F and $P/(P+V)$ with α_s and σ_q as free parameters. This fit gave α_s values between 0.14 and 0.17 with a mean value of 0.16. Therefore $\alpha_s = 0.16 \pm 0.04$ is independent of the fragmentation parameters.

The fragmentation parameters were then determined in a further analysis using events with low sphericity $S < 0.25$. This region is dominated by two jet events and is insensitive to α_s.

Simultaneous fits were made to: i) The x distribution ($x = p_h/E_b$). ii) The $\langle p_T^2 \rangle_{out}$ distribution. iii) The charged multiplicity distribution.

The fits yielded $a_F = 0.57 \pm 0.20$, $\sigma_q = 0.32 \pm 0.04$ GeV/c and $P/(P+V) = 0.56 \pm 0.15$ in agreement with the values found[60] earlier in lepton-hadron and hadron-hadron interactions. The quality of the fits is shown in Fig. 36. Using these parameter values as an input

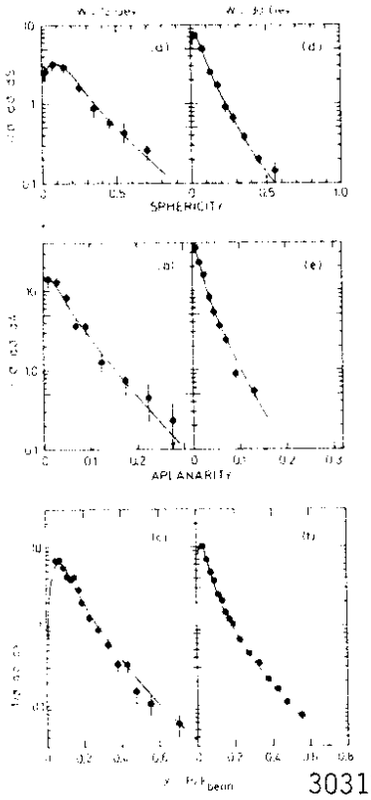

Fig. 36 - Comparison of the data with the QCD model (curves) at 12 GeV and 30 GeV in c.m.

to fit the events with $S > 0.25$ resulted in $\alpha_s = 0.17 \pm 0.02 \pm 0.03$.

Repeating the fit using the model of Hoyer et al.[58], gave

$$\alpha_s = 0.19 \pm 0.02.$$

This is expected since this model only considers two and three jet events whereas the second order model[59] also considers four jet events. The effective value of α_s in the first order model must thus be about 10% larger. However, remember that diagrams with internal gluon lines have been neglected[71].

The JADE group basically used the procedure outlined above to determine α_s. They find[12] $\alpha_s = 0.18 + 0.03 \pm 0.03$ consistent with an earlier[9] determination based on the planarity distribution.

The PLUTO group used the cluster method[11,64] described above to classify the events as two, three or four jet events. The value of α_s was then determined from the observed jet distribution. They find $\alpha_s = 0.15 \pm 0.03 \pm 0.02$.

It is clear that the values for α_s determined from the three jet events by various methods are in good agreement with a mean value $\alpha_s = 0.17$.

The value of α_s is related to Λ, the strong interaction mass scale (see Eq.8). It is still an open question what to use for q^2 in Eq.8. Maybe the best choice is $q^2 = p^2$, where p^2 is the quark-gluon effective mass squared. The p^2 distributions for the TASSO events with $S > 0.25$ are plotted in Fig. 37. Inserting the mean value $\langle p^2 \rangle = 140$ GeV^2 into the expression for $\alpha_s(q^2)$ yields

$\Lambda = (95^{+65}_{-35})$ MeV for $\alpha_s = 0.17 \pm 0.02$.

Including the systematic error yields $\Lambda < 290$ MeV.

From deep inelastic lepton hadron interactions values[40] for Λ between 100 and 500 MeV are found.

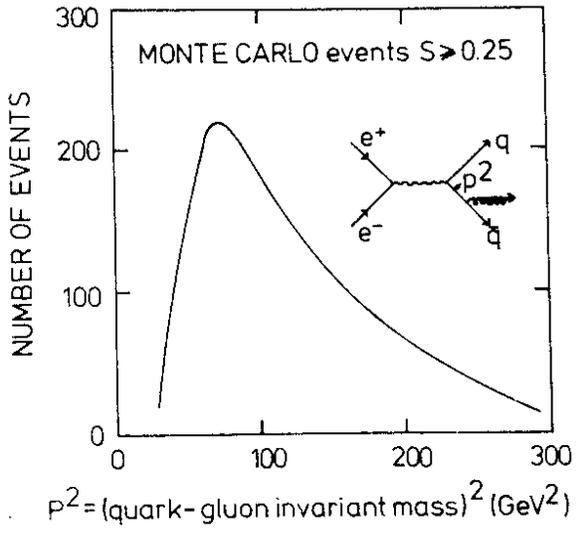

Fig. 37 - Distribution of the square of the quark-gluon mass as computed for events with large sphericity.

VI.4 SOFT GLUON EMISSION

So far we have primarily considered effects due to the emission of a single hard gluon at large angles. However, in the quark-gluon cascade leading to the final hadron jet most gluons are soft and emitted at small angles. The coupling constant α_s will thus be of order unity and many diagrams must be summed. It has been proposed[72] to relate the parton angular distribution within the cascade to two particle differential cross section:

$$1/\sigma \frac{d\sigma}{d\Omega} = \sum_{a,b} \int dz_a \int dz_b \cdot z_a \cdot z_b \frac{1}{\sigma} \frac{d^3\sigma}{dz_a \cdot dz_b \cdot d\Omega} \qquad (19)$$

where a and b are any two particles emitted in the event with normalized momenta z_a, z_b ($z = p/p_{beam}$) and an opening angle of $\pi-\theta$.

The PLUTO collaboration has determined[73] the two particle differential cross section for c.m. energies between 9.4 GeV and 31.6GeV. The data at 9.4 GeV and 31.6 GeV are plotted in Fig. 38 versus θ for small angles - i.e. the particles belong to opposite jets. The dashed

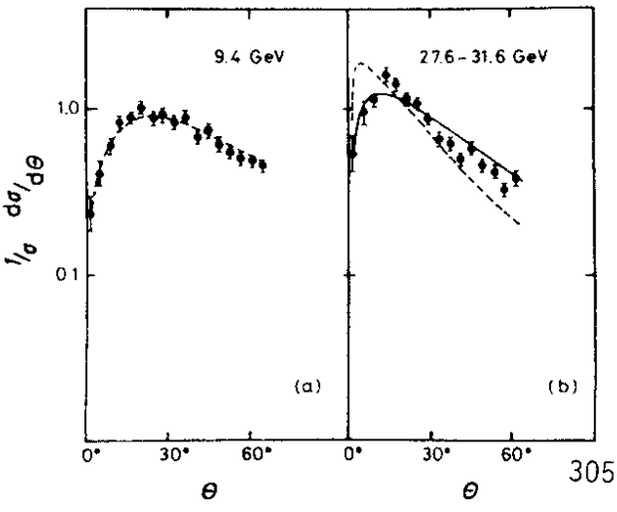

Fig. 38
$1/\sigma d\sigma/d\Omega$ measured by PLUTO plotted versus θ. The dashed and solid curves represent theoretical fits to the data.

curve represents a theoretical fit[74] to the data without hadronization. The fit is based on the QCD leading logarithmic approximation which is used to evaluate the fragmentation function for a parton a to produce a parton b. The parameters were determined from the 9.4 GeV data and used to predict the cross section at 30 GeV. The trend of the data is reproduced by this fit, however, the fit was much improved by including the hadronization of the partons shown as the solid line.

VI.5 DO QUARKS AND GLUONS FRAGMENT DIFFERENTLY ?

A gluon may fluctuate into pairs of quarks and gluons. Furthermore the ggg coupling is 9/4 times stronger than the $q\bar{q}g$ coupling such that gluon emission is expected to be more frequent for gluons than for quarks. This leads us to expect that a gluon and a quark will fragment into hadrons differently - the hadron spectrum from a gluon fragmentation will be softer with a correspondingly higher multiplicity.

Anderson, Gustafson and collaborators have suggested[75] studying

the yields of low-energy particles emitted at large angles with respect to the jet axis. The JADE group has carried out this analysis using charged and neutral particles. Planar events with $Q_2 - Q_1 > 0.10$ were divided into a slim jet and a broad jet by the plane normal to the thrust axis. The broad jet is then boosted into its own rest system and the particles assigned to the two subjets. The softest jet is called the gluon jet. Monte Carlo calculations imply that this is true about 70% of the time and it simply reflects the softness of a bremsstrahlung spectrum. All the particles are then projected on to the plane defined by T, thrust axis of the event and T* the thrust axis of the boosted two jet system. They then plot the particle densities between the gluon jet and the slim jet and the quark jet and the slim jet in terms of normalized angles θ_j/θ_{max}, where θ_{max} is the opening angle between the gluon jet and the slim jet or the quark jet and the slim jet respectively. The data plotted in Fig. 39 show that the density of tracks is larger by a factor of 2 between the slim jet and the quark jet. The result of a Monte Carlo computation based on similar fragmentation functions for quarks and gluons fails to reproduce the dip observed in the particle density distribution between the quark and the slim jet, as shown by the dotted histogram in Fig. 39. The data, however, can be reproduced by assuming that the quark has a harder fragmentation function than the gluon jet, as shown by the solid histogram. This may be a first experimental indication that quarks and gluons fragment differently.

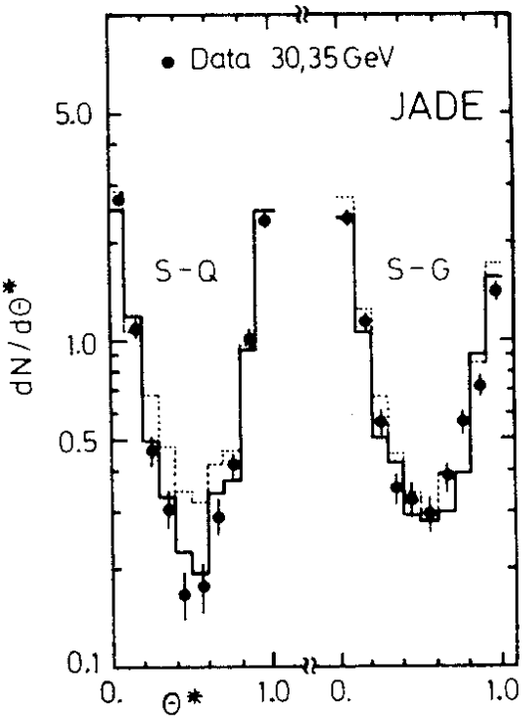

Fig. 39 - Angular distribution of charged particles between the slim jet and the gluon jet and between the slim jet and the quark jet as a function of the normalized angles θ/θ_{max}.

VII. TWO PHOTON INTERACTIONS

Electron-positron collisions are also a source of photon-photon collisions[76] as shown in Fig. 40, where the mass and the energy of the

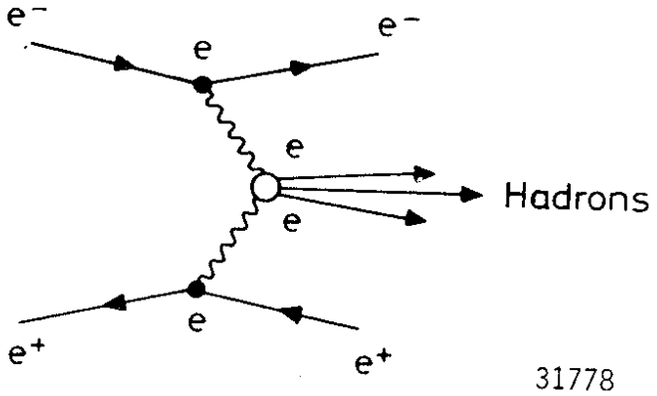

Fig. 40
Hadron production in $e^+e^- \to e^+e^- X$

spacelike photon is determined from a measurement of the scattered lepton. These processes offer a unique opportunity to vary the mass of the target and the projectile over a wide range from collisions of two nearly real photons via deep inelastic electron scattering on a photon target to collisions of two heavy photons.

Experimentally, two photon events are separated from annihilation events by a cut on the observed energy. The c.m. energy of the $\gamma\gamma$ system is in general much lower than the available energy, reflecting the product of two bremsstrahlungsspectra. The background from beam-gas events is rather low as determined from the number of events which satisfy the selection criteria but originates outside of the interaction point.

VII.1 RESONANCE PRODUCTION

All hadrons with even charge conjugation and spin different from one can be produced[77] in real $\gamma\gamma$ collisions.

The MARK II Collaboration at SPEAR has published[78] data on $e^+e^- \to e^+e^-\eta'$. They found a clean η' signal in the channel $\eta' \to \rho\gamma$ which gave $\Gamma^{\eta'}_{\gamma\gamma} = (5.8 \pm 1.1)$ keV with a systematic uncertainty of 20%. With the measured branching ratio of $BR(\eta' \to \gamma\gamma) = (2.0 \pm 0.3)\%$ this yields a total width $\Gamma^{tot}_{\eta'} = (293 \pm 76 \pm 59)$ keV in good agreement with the value of (280 ± 100) keV determined[79] by D.M.Binnie et al. from the reaction $\pi p \to \eta' n$ near threshold.

Events of the type $e^+e^- \to e^+e^-t^+t^-$ have been selected by PLUTO and TASSO at PETRA and by MARK II and the San Diego group at SPEAR to search for $\gamma\gamma$ production of resonances decaying into pairs of charged hadrons. The effective mass distribution of untagged two prong events determined by the PLUTO group[80] is plotted in Fig. 41 assuming the particles to be pions. The data show a broad maximum near 1.2GeV decreasing steeply towards higher masses. The bulk of the two prong events results from QED reactions $e^+e^- \to e^+e^-$ $(e^+e^- + \mu^+\mu^-)$ with an amplitude proportional to e^4. (In addition there is a small contribution from $\pi^+\pi^-$ Born events). This contribution has been evaluated[81]

and is shown as the solid line in Fig. 41.

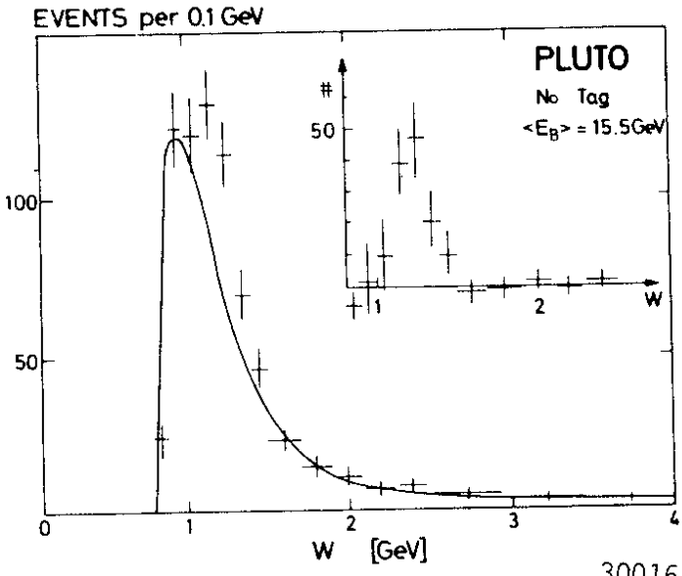

Fig. 4

Fig. 41 - Untagged two prong events from PLUTO plotted versus the pair mass. The solid line shows the QED contribution. The difference between the measured two prong yield and the QED contribution is shown

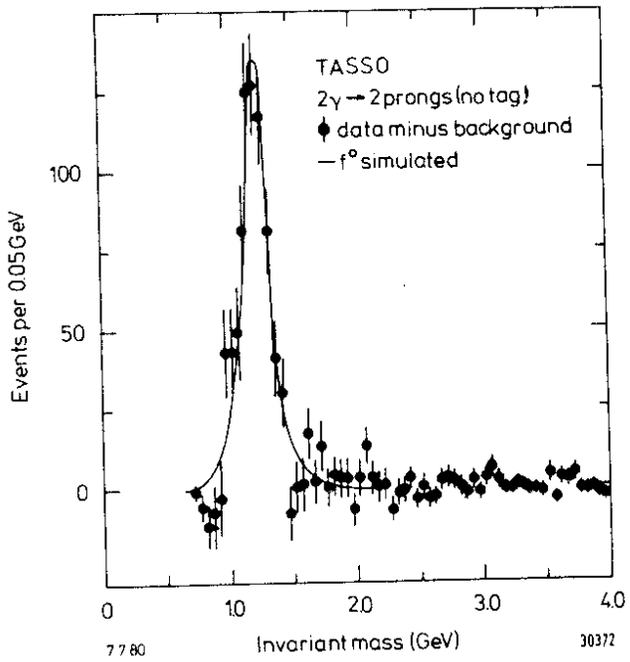

It describes all the data except for an excess near 1.25 GeV. The difference between the observed distribution and the QED prediction is a peak near 1.25 GeV as shown in the insert. It is natural to associate this peak with f^0 production since the f^0 has a mass of 1.27 GeV and decays into a $\pi^+\pi^-$ pair 83% of the time. A fit to the data assuming the f^0 to be produced with a helicity amplitude $\Lambda = 2$ gave $\Gamma^{f^0}_{\gamma\gamma} = (2.3 \pm 0.5 \pm 0.35)$ keV there the first error is statistical and the second systematic.

The two prong mass distribution obtained[13,82] by TASSO with the QED contribution subtracted is plotted in Fig. 42. The data show a clear peak at 1.25 GeV which yields a preliminary value of $\Gamma^{f^0}_{\gamma\gamma} = (4.1 \pm 0.4 \pm 0.6)$ keV for $\Lambda = 2$, barely consistent with the PLUTO value.

Fig. 42

Untagged two prong events from TASSO plotted versus the pair mass with the QED background subtracted. The data are preliminary.

Preliminary data[83] from MARK II are shown in Fig. 43 where the number of untagged two prong events is plotted versus the the pair mass. The QED contribution has been subtracted. Again a clear enhancement is seen at a mass around 1.2 GeV. However, the enhancement is not well fit by a single Breit-Wigner resonance and hence no value is quoted for the radiative width.

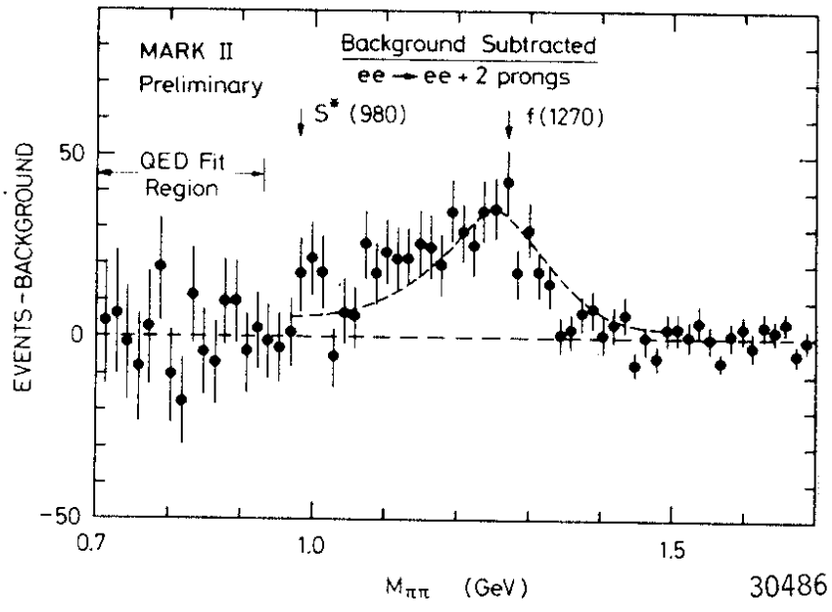

Fig. 43
Untagged two prong events from MARK II Collaboration at SPEAR plotted versus the pair mass with the QED background subtracted. The data are preliminary.

The San Diego group[84] using tagged events found 21 events above the QED background centered around the f mass. Assigning these events to $e^+e^- \to e^+e^- f^0$ yields $\Gamma^{f^0}_{\gamma\gamma} = 9.5 \pm 3.9 \pm 2.4$ keV assuming $\Lambda = 2$.

VII.2 OBSERVATION OF $e^+e^- \to e^+e^- \rho^0\rho^0$

The TASSO group reports[14,85] results on $\gamma\gamma \to \rho^0\rho^0$. The $\rho^0\rho^0$ cross section was extracted from the data by selecting neutral, four prong events with the sum of the transverse momentum with respect to the beam axis less than 0.15 GeV. The invariant $\gamma\gamma$ mass was required to be between 1.5 and 2.3 GeV. This results in 89 events, with a negligible background from beam gas events. They estimate one event from one photon annihilation and 15 events from events containing additional unobserved particles.

The cross section for $\gamma\gamma \to \rho^0\rho^0$ is plotted in Fig. 44 versus the c.m. energy of the $\gamma\gamma$-system. The cross section peaks strongly near threshold and drops rapidly with energy in disagreement with a simple V.D.M. asymptotic prediction. However close to threshold nonasymptotic effects are expected to be important

VII.3 HADRON PRODUCTION WITH REAL PHOTONS

The amplitude for $\gamma\gamma \to$ hadrons will presumably contain both the hadronlike[86] piece and the pointlike[87] piece shown in Fig. 45. In the

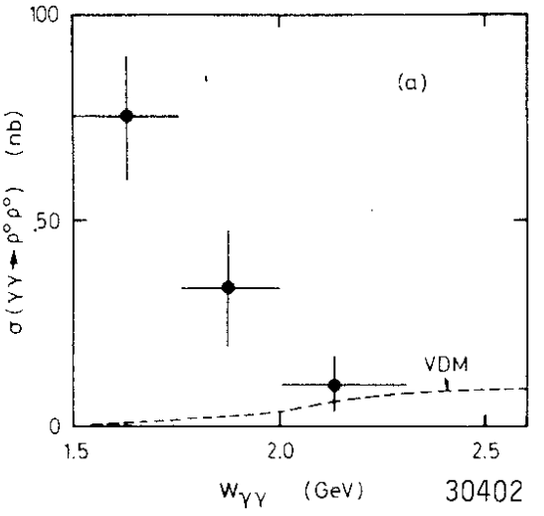

Fig. 44 - Cross section for $e^+e^- \to e^+e^-\rho^0\rho^0$ as measured by TASSO. An asymptotic VDM prediction is shown as the dotted line.

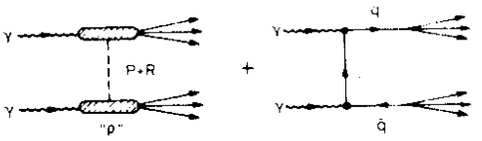

Fig. 45
The hadronlike and the pointlike contribution to $\gamma\gamma \to$ hadrons

hadronic piece the photons convert into vector mesons which subsequently interact producting a final state similar to that produced in hadron hadron collisions, where the secondary hadrons tend to be produced with low transverse momenta with respect to the beam axis. In addition, however, the photon has a pointlike piece where the photon couples directly to a quark pair initiating a hard scattering process. In this case the secondary hadrons will appear in two jets of hadrons distributed roughly as $1/p_T^4$ with respect to the beam axis.

The total cross section for $\gamma\gamma \to$ hadrons can be estimated from the imaginary part of the elastic scattering amplitude to

$$\sigma(\gamma\gamma \to \text{hadrons}) = 240 \text{ nb} + \frac{270 \text{ nb GeV}}{W} + \frac{C \text{ nb GeV}^2}{W^2} \qquad (20)$$

The first term results from Pomeron exchange and was estimated from factorization $\sigma_{\gamma\gamma} \cdot \sigma_{pp} = (\sigma_{\gamma p})^2$. The second term involves f_2 and A_2 exchange and leads to a cross section which decreases as $1/W$ where W is the energy of the hadronic system. The pointlike contribution is expected to decrease roughly as $1/W^2$.

The total hadronic cross section has been measured[13] both by the PLUTO and the TASSO Collaboration. Both groups collected data by detecting only one of the electrons leaving the other untagged. The total energy W of the produced hadron system was estimated from energy W_{vis} observed in the detector. Only charged particles were observed in TASSO whereas PLUTO also measured photons. The observed cross sections were extrapolated to $Q^2 = 0$ using the ρ-propagator:

$$\sigma_{\gamma\gamma}(W) = \sigma_{\gamma\gamma}(W,Q^2) \cdot \left[\frac{m_\rho^2}{m_\rho^2 + Q^2}\right]^{-2} \qquad (21)$$

Note that this simple Ansatz violates scaling and is not valid in electroproduction at large values of Q^2. The Q^2 dependence of the total cross section is shown in Fig. 46 together with the ρ-propagator fit.

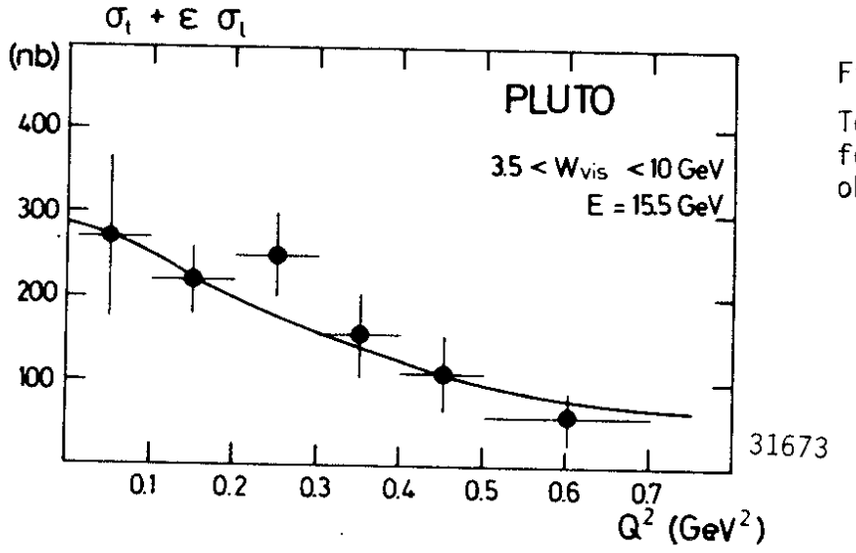

Fig. 46

Total cross section for $\gamma^*\gamma \to$ hadrons observed by PLUTO.

The cross sections extrapolated to $Q^2 = 0$ are plotted versus W in Fig. 47. The VDM contribution is also shown as the dotted line. Note that the TASSO data are preliminary.

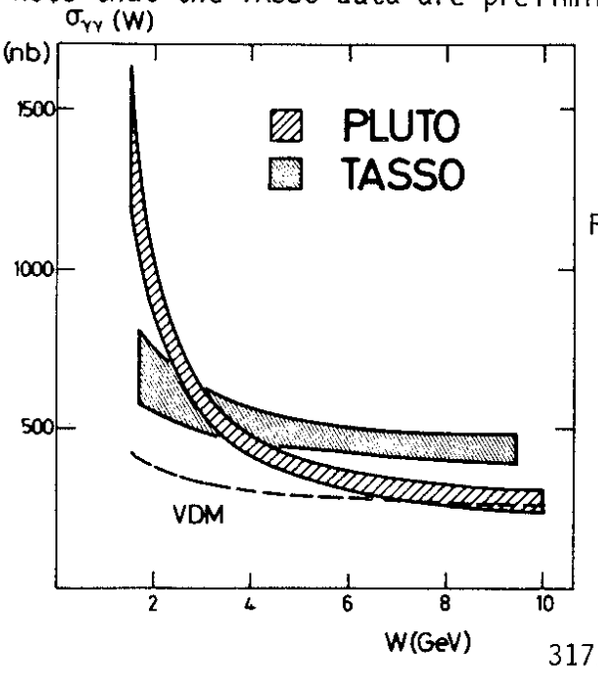

In addition to the statistical errors indicated by the bands, there are systematic errors of 15% and 25% for the PLUTO and the TASSO data respectively.

Fig. 47 - The total cross section for $\gamma\gamma \to$ hadrons plotted versus the mass of the produced hadron system. Note that the TASSO data are preliminary and that only statistical errors are shown.

The data from the two groups are marginally consistent within the errors. However, the PLUTO cross section clearly decreases steeper with energy than the TASSO cross section does:

A best fit to the PLUTO data gives:

$$\sigma_{\gamma\gamma} = A \left(240 \text{ nb} + \frac{270 \text{ nb GeV}}{W}\right) + \frac{B \text{ nb GeV}^2}{W^2} \qquad (22)$$

$$A = 0.97 \pm 0.16 \quad \text{and} \quad B = 2250 \pm 500$$

whereas the TASSO data are fit by

$$\sigma_{\gamma\gamma} = 380 \text{ nb} + \frac{520 \text{ nb} \cdot \text{GeV}}{W} \qquad (23)$$

Although, the PLUTO data might suggest the presence of a pointlike term they clearly do not yet prove it. The pointlike contribution might show up more clearly in the transverse momentum distribution of the hadrons at large values of p_T were the hadron-like contribution has disappeared.

The transverse momentum distribution measured by PLUTO is plotted in Fig. 48 versus p_T^2. The spectrum drops rapidly at small values of p_T^2 and flattens at large values of p_T^2 where indeed the slope is consistent with $1/p_T^4$ as expected for the hard component. The solid line represents the contribution from the pointlike diagram.

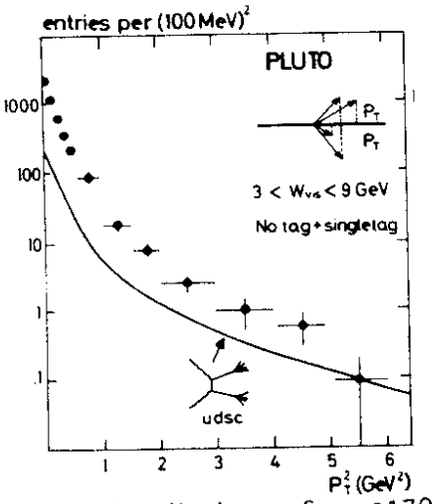

Fig. 48 - Number of tracks plotted versus the square of the transverse momentum with respect to the beam axis. The solid curve is a prediction based on $\gamma\gamma \to q\bar{q} \to$ hadrons with q =u,d, s, c quarks.

31702

A candidate for a hard scattering event obtained by PLUTO is shown in Fig. 49. When viewed along the beam direction the event appears as two collinear jet of hadrons. When viewed transverse to the beam direction the event is seen to have a unbalanced longitudinal momenta as expected for a $\gamma\gamma$ event.

The PLUTO group has determined the two jet axes in such an event by maximizing the thrust of the event using two independent axes. It is interesting to note[88] that the mean p_T of the hadrons computed with respect to these axes is 300 MeV.

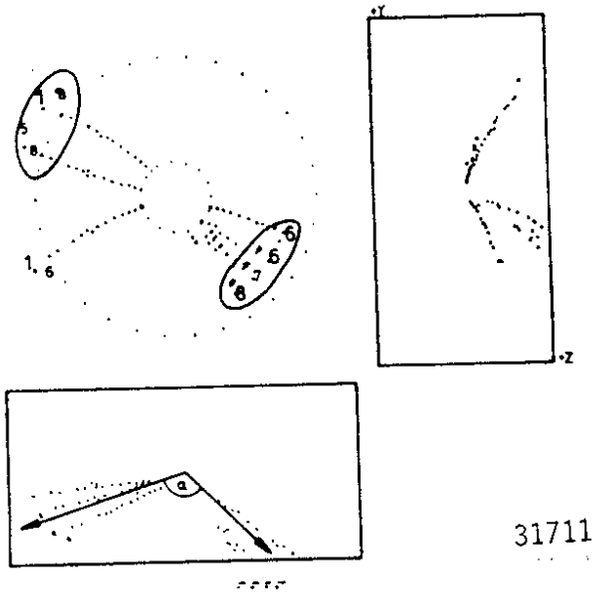

Fig. 49 - Candidate for $\gamma\gamma \to q\bar{q} \to$ hadrons observed by PLUTO.

31711

The properties of these events are strongly suggestive of a pointlike production mechanism . However, it should be remembered that ordinary one photon annihilation events with radiation in the initial state could lead to events with the same topology. This mechanism , however, can be excluded if the electron is tagged on the same side as the direction of the longitudinal momentum vector of the jets. The PLUTO group finds the expected number of 2-jet events with the tagged electron on the same side as the momentum vector, appearantly excluding this background source.

VII.4 ELECTRON SCATTERING ON A PHOTON TARGET

The PLUTO Collaboration reports[13] the first data on deep inelastic electron-photon scattering. These data were collected by tagging one electron at scattering angles between 70 mrad and 250 mrad corresponding to values of Q^2 between 1 $(GeV/c)^2$ and 15 $(GeV/c)^2$ with a mean value of 5 $(GeV/c)^2$. The second electron was not detected yielding a nearly real target photon. A total of 120 multihadron events with this electron topology were observed.

Deep inelastic electron-photon scattering[89] as shown in Fig.50 can be parametrized in terms of three structure functions. $F_1(x,Q^2)$ and $F_2(x,Q^2)$ corresponds to the longitudinal and to the transverse polarisation vector of the virtual photon respectively and $F_3(x,Q^2)$ to the transverse polarisation vector of the target photon in the scattering plane. $x = Q^2/(Q^2+W^2)$ and W is the mass of the hadronic system. $F_3(x,Q^2)$ will average to zero since the scattering plane was not determined. Furthermore $F_L(x,Q^2)$ is expected to be smaller than $F_2(x,Q^2)$ and the PLUTO group therefore analyze their data in terms of $F_2(x,Q^2)$ only.

Both the hadronlike part and the pointlike part of the photon contributes to $F_2(x,Q^2)$ as indicated in Fig. 50b,c. In the hadronlike part the photon transforms into a vector meson and the virtual photon interacts with the quarks in the vector meson. This contribution cannot be calculated from first principles but it will have an x dependence similar to that observed in the structure function of the pion i.e. $F_2(x,Q^2)_{VDM} \sim (1-x)^{c_1+c_2 \ln(\ln Q^2)}$ and, just like lepton-hadron interactions, only its evolution with Q^2 is predicted in QCD. The pointlike piece (50c) can be calculated to all orders in a perturbation theory. The lowest order calculation gives:

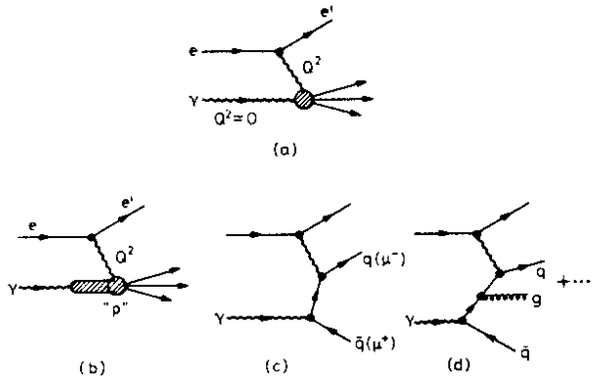

Fig. 50 - Diagrams contributing to $e\gamma \to e'$hadrons.

$$F_2(x,Q^2)_{point} = \frac{\alpha}{\pi} \sum_i e_i^4 \, x(x^2 + (1-x)^2) \cdot \ln Q^2/\Lambda^2. \qquad (24)$$

The pointlike contribution leads to a structure function which peaks at large values of x, whereas the VDM piece leads to a structure function which is large at small x and disappears at large x. The lowest order pointlike contribution is indeed proportional to the QED process $e^+e^- \to e^+e^- \mu^+\mu^-$.

Higher order QCD corrections (Fig. 50d), including the emission of soft gluons, will soften the Born spectrum by depleting the density of fast quarks and enchancing the density of slow quarks.

The values for $(1/\alpha)F_2(x)$, extracted from the hadron data, are plotted in Fig. 51a versus x and compared to the formfactor observed in the QED process $e^+e^- \to e^+e^- (e^+e^- + \mu^+\mu^-)$ (Fig. 51b). Both structure functions peak at large x demonstrating the existence of the pointlike piece. The Born prediction, shown as the solid curve, follows the general trend of the data quite well.

The evoluation of the formfactor with increasing Q^2 will make it possible to determine Λ with good precision in a high statistics experiment. The simplicity of the target, with no finite mass effects and no higher twist effects caused by a premordial p_T distribution, makes it possible to determine Λ without the systematic uncertainties which have beset the determination in deep inelastic lepton-hadron processes. In particular it may be possible to use data in a Q^2 range such that the variation in $\ln Q^2/\Lambda^2$ are still quite large.

31701

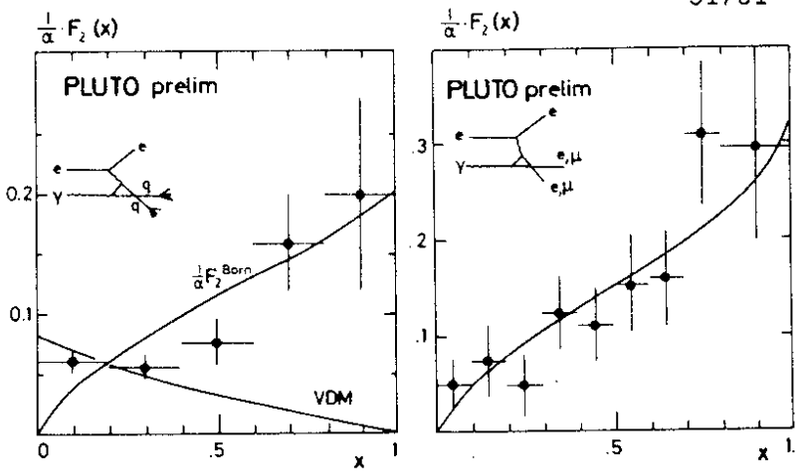

Fig. 51

The structure functions of the photon (a) and the lepton (b).

I would like to thank my scientific secretaries J.Cleymans, D.Haidt and G.Zobernig and all the speakers on the PETRA data at Wisconsin for their help and support. I'm grateful to J.Ellis, J. Freeman, T.Meyer, H.L.Lynch, T.F.Walsh, G.Wolf, S.L.Wu for support and discussions.

DISCUSSIONS

Q.E.L.Berger (Argonne)

Do you have any information on the energy dependence of the very interesting back-to-back charge correlation which you showed ? Is it growing or falling with Q^2? It could be an inverse power $1/Q^2$ higher twist effect.

A. At present only the high energy data have sufficient statistics to establish the charge correlation effect.

Q. B.Barnett (John Hopkins Univ.)

In your charge correlation data, have you taken into account the fact that once you have chosen a positive particle there is an extra negative particle somewhere due to charge conservation. This effect will give an apparent correlation about the size you see, and, therefore your claim of seeing a positive effect is probably premature.

A. May be I didn't make myself clear. What we do is to pick a charge at a certain y. The remaining event is then of course oppositly charged and the question which we try to answer is how this compensating charge is distributed as a function of rapidity. If you pick the test particle at $y \sim 0$, then also the compensating charge is centered at $y = 0$. If the test particle has a large value of y then a significant part of the charge compensation is done by particles far removed in rapidity - i.e. they belong to the opposite jet.

Q. D.S.Narayan (Tata Institute, India)

1) Comment on oblateness events: At 12 GeV, Monte Carlo produces planar events in agreement with expectations. These planar events in Monte-Carlo are planar due to fluctuations. The fluctuations depend on the input parameters in the Monte Carlo. At 30 GeV, the Monte Carlo does not give adequate number of events. Does this show the existence of the gluon ? Or may be the inputs on the Monte Carlo are unrealistic.

2) Comment on charge correlation. Charge correlation (+, -) of the fastest particles on the opposite sides is partly kinematical since that charge = 0. An more appropriate thing to do is to look to the charge correlations of the fastest and next to fastest particles on the same side. In deep inelastic scattering, the uncorrelated Monte Carlo explains the data well but the parametrization of Feynman and Field give the wrong trend.

A.1) Indeed the data at low energeis can be well fit in terms of $e^+e^- \to q\bar{q}$ and this can be used to determine the parameters for the quark fragmentation. This is not possible at high energies. The $q\bar{q}$ model cannot reproduce the observed final state for any values of the parameters in the Monte Carlo program. However, the data are very naturally explained as gluon bremsstrahlung with only a single new parameter α_s the strength of the coupling between a quark and a gluon.

2) See the answer given to Prof. Barnett.

Q. N.K.Yamdagni (Univ. of Stockholm, Sweden)
In view of fact the fraction of energy going to charged particles is varying significantly, perhaps the average charged multiplicity should be given as a function of the fraction of energy going in the charged mode.

Q. V.Lüth (SLAC)
How do you separate the untagged 2 jet events from 2γ interaction from background due to initial state radiation. How big is this background ? How do you measure the contribution ?

A. This is indeed one of the problems since radiation in the initial state will lead to the same topology as $e^+e^- \to e^+e^- q\bar{q}$ events. However this contribution can be computed and subtracted and the PLUTO group claim it is a small contribution. A collinear two jet events where an electron is tagged on the same side as the direction of the momentum vector of the two jets cannot result from radiation in the initial state. PLUTO claim to find the correct number of such events.

Q. A.Roussarie (SLAC)
About the $\gamma\gamma$ production of $\pi\pi$ resonances. We are not quoting a limit on the partial width $\Gamma f^0 \to \gamma\gamma$ because as you have shown the $\pi\pi$ mass spectrum is not compatible with only f production. We think that we subtract the continuum in a better way than in PETRA because our spectrum begins at 0.6 GeV of mass and the PETRA spectrum due to the trigger begins only at 1 GeV. They may have acceptance problems.

A. Being able to measure down to 0.6 GeV is clearly an advantage. However, the DESY group do have a few points below the f mass and these observed cross sections can be explained by QED production only.

REFERENCES:

1) A.Böhm, Minirapporteur talk in section C8, XXth International Conference on High Energy Physics, July 17-23, 1980, University of Wisconsin, Madison, Wisconsin.
2) D.Cords, Minirapporteur talk in section C2, XXth International Conference on High Energy Physics, July 17-23, 1980, University of Wisconsin, Madison, Wisconsin.
3) D.Pandoulas, Minirapporteur talk in section C2, XXth International Conference on High Energy Physics, July 17-23, 1980, University of Wisconsin, Madison, Wisconsin.

4) S.L.Wu, Minirapporteur talk in section C2, XXth International Conference on High Energy Physics, July 17-23, 1980, University of Wisconsin, Madison, Wisconsin.
5) B.H.Wiik, Proceedings of the International Neutrino Conference, Bergen, Norway, June 1979, p. 113
P.Söding, Proceedings EPS International Conference on High Energy Physics, Geneva, Switherland, July 1979, p. 271
6) TASSO-Collaboration, R.Brandelik et al., Phys.Lett. 83B,261 (1979)
7) MARK J Collaboration, D.P.Barber et al.,Phys.Rev.Lett.43,830(1979)
8) PLUTO Collaboration,Ch.Berger et al.,Phys.Lett.86B,418(1979)
9) JADE Collaboration, W.Bartel et al., Phys.Lett.91B,142 (1980)
10) MARK J Collaboration, H.Newmann, Minirapporteur talk in section C3, XXth International Conference on High Energy Physics, July 17-23, 1980, University of Wisconsin, Madison, Wisconsin
11) PLUTO Collaboration, V.Hepp, Minirapporteur talk in section C3, given at the XXth International Conference on High Energy Physics, July17-23, 1980, University of Wisconsin, Madison, Wisconsin.
12) JADE Collaboration, S.Yamada, Minirapporteur talk in section C3, given at the XXth International Conference on High Energy Physics, July 17-23, 1980, University of Wisconsin, Madison, Wisconsin.
13) W.Wagner, Minirapporteur talk in section C1, XXth International Conference on High Energy Physics, July 17-23, 1980, University of Wisconsin, Madison, Wisconsin.
14) E.Hilger, Minirapporteur talk in section C1, XXth International Conference on High Energy Physics, July 17-23, 1980 University of Wisconsin, Madison, Wisconsin.
15) F.A.Berends, K.J.F.Gaemers and R.Gastmans, Nucl.Phys.B57,381(1973), Nucl.Phys.B63, 381 (1973) and Nucl.Phys. B68, 541 (1979)
F.A.Berends and G.J.Komen, Phys.Lett. 63B, 432 (1976) and private communication F.A.Berends and R.Kleiss.
16) H.Salecker, Zeitschr. für Naturforschung 8a, 16 (1953) and 10a, 349 (1955)
S.D.Drell, Ann.Phys. 4, 75 (1958)
T.D.Lee and G.G.Wick, Phys.Rev. D2, 1033 (1970)
17) J.A.McClure and S.D.Drell, Nuovo Cim. 37, 1638 (1965)
N.M.Kroll, Nuovo Cim. 45A, 65 (1966)
18) A.Litke, Harvard University, Thesis 1970
19) JADE Collaboration, W.Bartel et al., Phys.Lett. 92B, 206 (1980)
MARK J Collaboration, D.P.Barber et al., Phys.Rev.Lett.42,1110(1979) and 43, 1915 (1979) and Phys.Lett.95B, 149 (1980)
PLUTO Collaboration, Ch.Berger et al.,Z.Physik C4, 269 (1980) and Phys.Lett. 94B, 87 (1980)
TASSO Collaboration, R.Brandelik et al., Phys.Lett.92B, 199 (1980) and 94B, 259 (1980)
20) S.L.Glashow, Nucl.Phys.22, 579 (1961)
S.Weinberg, Phys.Rev.Lett. 19, 1264 (1967)
A.Salam, Proc. 8th Nobel Symposium, N.Svartholm editor, Wiley NY 1968
21) J.Ellis and M.K.Gaillard, CERN 76-18
22) N.Wright and J.J.Sakurai, Phys.Rev. D22, 220 (1980)
23) H.Georgi and S.Weinberg, Phys.Rev.D17, 275 (1978)
J.D.Bjorken, Phys.Rev. D19, 335 (1979)

24) JADE Collaboration, R.Marshall, Private communication.
25) MARK J Collaboration, D.P.Barber et al., RWTH Aachen, PITHA Preprint 80/08 1980
26) E.H.de Groot, G.J.Gounaris and D.Schildknecht, Phys.Lett.85B,399(1979) Phys.Lett.90B,427 (1980) and Z.für Physik C5, 127 (1980)
27) V.Barger, W.Y.Kenny and E.Ma, Wisconsin-Hawai-Reports UW-COO-881-126(1980); US-COO881-133 (1980) and UW-COO-881-138 (1980)
28) MARK J Collaboration, MIT, Technical Report No. 113, 1980 TASSO Collaboration, R.Brandelik et al., in preparation.
29) P.Fayet and S.Ferrara, Phys.Reports 32C, 249 (1977) P.Fayet, Phys.Lett. 69B, 489 (1977) G.R.Farrar - Proc.Int.School of Subnuclear Physics, Erice,Italy, Aug. 1978 G.R.Farrar and D.Fayet, Phys.Lett. 76B, 578 (1970) and 79B,442 (1970) G.R.Farrar and D.Fayet, Searching for the spin 0 leptons of supersymmetry Rutgers / Caltech preprint 1979 G.Barbellini et al., ECFA/LEP Study Group, DESY Preprint 79/67
30) Yu. A.Gal'fand and E.P.Likhtman, JETP Letters 13, 323 (1971) D.V.Volkov and V.P.Akulov, Phys.Lett. 46B. 109 (1973) J.Wess and B.Zumino Nucl.Phys.B70,39(1974)
31) S.D.Drell, D.J.Levy, and T.M.Yan, Phys.Rev.187, 2159 (1969) and Phys.Rev.D1, 1617 (1970)
32) N.Cabibbo, G.Parisi, and M.Testa, Lett.Nuovo Cimento 4,35 (1970)
33) J.D.Bjorken and S.J.Brodsky, Phys.Rev. D1, 1416 (1970)
34) R.P.Feynman, Photon-Hadron Interactions (Benjamin, Reading Mass., p.166 (1972)
35) R.F.Schwitters et al., Phys.Rev.Lett. 35, 1230 (1975) G.G.Hanson et al., Phys.Rev.Lett. 35, 1609 (1975) G.G.Hanson, Proceedings of 13th Rencontre de Moriond, edited by J.Tran Thanh Van, Vol II, p.15 and SLAC-PUB 2118 (1978) PLUTO Collaboration, Ch.Berger et al., Phys.Lett.B78, 176 (1978)
36) J.Kogut and L.Susskind, Phys.Rev.D9, 697 , 3391 (1974) A.M.Polyakov, Proceedings of the 1975 International Symposium on Lepton and Photon Interactions at High Energies, Stanford, Aug. 21-27, 1975
37) The first quantitative discussion on the experimental implications of gluon bremsstrahlung in e^+e^- annihilation was given by: J.Ellis, M.K.Gaillard and G.G.Ross, Nucl.Phys. B111,253 (1976) - erratum B 130, 516 (1977)
38) T.A.DeGrand, Yee Jack Ng, and S.-H.H.Tye, Phys.Rev.D16, 3251 (1977) A.de Rujula, J.Ellis, E.G.Floratos and M.K.Gaillard, Nucl.Phys.B 138, 387 (1978) G.Kramer and G.Schierholz, Phys.Lett. 82B, 102 (1979) G.Kramer, G.Schierholz and J.Willrodt, Phys.Lett.79B,249 (1978) P.Hoyer, P.Osland, H.G.Sander, T.F.Walsh and P.M.Zerwas, Nucl.Phys. B 161, 349 (1979) G.Kramer, G.Schierholz and J.Willrodt, Z.für Physik C4,149 (1980)
39) H.Fritzsch, M.Gell-Mann and H.Leutwyler, Phys.Lett. 47B,365(1973) D.J.Gross and F.Wilczek,Phys.Rev.Lett. 30, 1343 (1973) H.D.Politzer, Phys.Rev.Lett. 30, 1346 (1973) S.Weinberg, Phys.Rev.Lett. 31, 31 (1973)

H.D.Politzer, Phys.Reports 19, 129 (1979)
W.Marciano and H.Pagels, Phys.Reports. 36, 137 (1978)
40) See reports given at the XX International Conference on High Energy Physics, Madison, Wisconsin, July 17-23, 1980
41) S.Brandt et al., Phys.Lett. 12, 57 (1969)
E.Farhi, Phys.Rev.Lett. 39, 1587 (1977)
S.Brandt and H.D.Dahmen, Z.Physik C1, 61 (1979)
42) A.Quenzer, thesis, Orsay Report LAL 1299 (1977)
A.Cordier et al., Phys.Lett. 81B, 389 (1979)
V.A.Sidorov, Proceedings of the XVIIIth International Conference on High Energy Physics, Tbilisi, USSR, B 13 (1976)
R.F.Schwitters, Proceddings of the XVIIIth International Conference on High Energy Physics, Tbilisi, USSR, B 34 (1976)
J.Perez-Y-Jorba, Proceedings of the XIXth International Conference on High Energy Physics, Tokyo, p.269 (1978)
PLUTO Collaboration, J.Burmester et al., Phys.Lett. 66B, 395(1977)
DASP Collaboration, R.Brandelik et al., Phys.Lett. 76B, 361 (1978)
43) T.Appelquist and H.Georgi, Phys.Rev. D8, 4000 (1973)
A.Zee, Phys.Rev. D8, 4038 (1973)
G.'t Hooft, Nucl.Phys. B 62, 444 (1973)
M.Dine and J.Sapirstein, Phys.Rev.Lett. 43, 668 (1979)
W.Celmaster and R.J.Gonsalves, UCSD Preprint UCSD-10P10-206,207(1979)
K.G.Chetyrkin, A.L.Kataev and F.V.Tkachov,Phys.Lett.85B,277(1979)
USSR Academy of Sciences, Institute of Nuclear Research Preprint D-0178 (1980)
44) TASSO Collaboration, R.Brandelik et al.,Phys.Lett.89B,418 (1980)
45) JADE Collaboration, W.Bartel et al.,Phys.Lett. 88B, 171 (1979)
46) PLUTO Collaboration, Ch.Berger et al., DESY Report 80/69 (1980)
47) C.Bacci et al., Phys.Lett. 86B, 234 (1979)
SLAC-LBL Collaboration, G.G.Hanson, 13th Rencontre de Moriond (1978) ed.by J.Tran Thanh Van, Vol. III - 1978
PLUTO Collaboration, Ch.Berger et al., Phys.Lett. 81B, 410 (1979) and V.Blobel private communication
DASP Collaboration, R.Brandelik et al., Nucl.Phys.B 148, 189 (1979)
48) W.Thomé et al., Nucl.Phys. B 129, 365 (1977)
See also review by E.Albini, P.Capiluppi, G.Giacomelli, and A.M.Rossi, Nuovo Cimento 32A, 101 (1976)
W.Thomé, Aachen preprint PITHA 80/4 (1980)
49) R.Stenbacka et al., Nuovo Cimento 51A, 63 (1979)
50) W.Furmanski, R.Petronzio and S.Pokorski, Nucl.Phys.B155,253 (1979)
A.Bassetto, M.Ciafaloni and G.Marchesini,Phys.Lett.83B,207 (1978)
51) K.Konishi, Rutherford Preprint RL 79-035 T 241 (1979)
52) G.J.Feldman and M.L.Perl, Phys.Reports 33, 285 (1977)
53) TASSO Collaboration, R.Brandelik et al., Phys.Lett.89B,418 (1980)
54) TASSO Collaboration, R.Brandelik et al., Phys.Lett.94B, 444 (1980)
55) TASSO Collaboration, R.Brandelik et al., Phys.Lett. 94B, 91 (1980)
56) V.Lüth et al., Phys.Lett. 70B, 120 (1977)
57) T.F.Walsh and P.Zerwas, Nucl.Phys. B 77, 494 (1974)
58) P.Hoyer, P.Osland, H.G.Sander, T.F.Walsh and P.M.Zerwas, Nucl.Phys. 161, 349 (1979)
59) A.Ali, E.Pietarinen, G.Kramer and J.Willrodt, Phys.Lett.93B,155(1980)

60) R.D.Field and R.P.Feynman, Nucl.Phys. B 136, 1 (1978)
61) The Lund Monte Carlo, T.Sjöstrand, B.Söderberg,
Lund Report LU TP 78-18 (1978)
T.Sjöstrand, Lund Report LU TP 79-8 (1979)
62) G.Altarelli and G.Parisi, Nucl.Phys. B 126, 298 (1977)
JADE-Collaboration, W.Bartel et al., Phys.Lett.91B,142 (1980)
63) Physics with High Energy, Electron-Positron Colliding Beams
with MARK J Detector, Physics Report 63, 340 (1980)
64) PLUTO Collaboration, Ch.Berger et al., DESY Report 80/93
H.J.Daum, H.Meyer and J.Bürger, DESY Report 80/101
65) S.L.Wu and G.Zobernig, Z.für Physik C2, 10) (1979)
66) JADE Collaboration, W.Bartel and A.Petersen, Talks given at the
XVth Rencontre de Moriond, Les Arcs, March 9-21, 1980
67) J.Ellis and I.Karliner, Nucl.Phys. B 148, 141 (1979)
68) TASSO Collaboration, R.Brandelik et al., DESY Report 80/80 (1980)
F.A.Berends and R.Kleiss - to be published.
69) MARK J Collaboration, D.P.Barber et al., Phys.Lett. 89B,139 (1979)
70) TASSO Collaboration, R.Brandelik et al., Phys.Lett. 94B, 437 (1980)
71) R.K.Ellis, D.A.Ross and A.E.Terrano, Caltech.Report 68-785 (1980)
Z.Kunszt, DESY Report 80/79 (1980)
K.Fabricius, I.Schmitt, G.Schierholz and G.Kramer,
DESY Report 80/79 (1980)
72) Yu.L.Dokshitzer, D.I. D'yakonov and S.I.Troyan,
Phys.Lett. 78B, 290 (1978)
73) PLUTO Collaboration, Ch.Berger et al., Phys.Lett. 90B, 312 (1980)
74) R.Baier and K.Fey, Univ. of Bielefeld preprint BI-TP 80/10 (1980)
75) B.Anderson and G.Gustavson, Lund Preprint LU TP 79-2 (1979)
B.Anderson and G.Gustafson, Z.für Physik C3, 223 (1980)
B.Anderson, G.Gustavfon and T.Sjöstrand, Lund Report LU TP80-1(1980)
B.Anderson, G.Gustafson and C.Peterson, Nucl.Phys.B135, 273 (1978)
76) E.J.Williams, Kgl.Danske Videnskab.Selskab, Mat.Fys.Medd.
13 No. 4 (1934)
L.Landau and E.Lifshitz, Physik Z, Sovjetunion 6, 244 (1934)
A.Jaccarini, N.Arteaga-Romero, J.Parisi and P.Kessler,
Compt.Rend. 269B, 153, 1129 (1969)
Nuovo Cimento 4, 933 (1970)
S.J.Brodsky, T.Kinoshita and H.Terazawa, Phys.Rev. D4,1532 (1971)
Phys.Rev.Lett.25, 972 (1970)
77) F.F.Low, Phys.Rev. 120, 582 (1960)
F.Calogero and C.Zemach, Phys.Rev.120, 1860 (1960)
78) G.S.Abrams et al., Phys.Rev.Lett. 43, 477 (1979)
79) D.M.Binnie et al., Imperial College London, NO IC/HENP/79/2 (1979)
80) PLUTO Collaboration, Ch.Berger et al.,Phys.Lett. 94B, 254 (1980)
81) J.A.M.Vermaseren, private communication
R.Bhattacharya, J.Smith and G.Grammer,Phys.Rev.D15, 3267 (1977)
82) E.Hilger, invited paper given at the International workshop on
$\gamma\gamma$ collisions, Amiens, April 8-12, 1975 France
DESY Report 80/75, Bonn-HE-80/5
83) A.Roussarie, Minirapporteur talk in section C1, XXth International
Conference on High Energy Physics, July 17-23, 1980 University
of Wisconsin, Madison, Wisconsin.

84) C.J.Biddick et al., Paper submitted to the Wisconsin Conference
85) TASSO Collaboration, R.Brandelik et al., DESY Report 80/77
86) J.J.Sakurai, Ann.Phys. 11, 1 (1960)
87) S.M.Berman, J.D.Bjorken and J.B.Kogut
Phys.Rev. D4, 3388 (1971)
S.J.Brodsky, F.E.Close and J.F.Gunion, Phys.Rev.D5,1384(1972)
88) H.Spitzer, talk given at the XV Recontre de Moriond, Les Arcs, France, March 15-21, 1980
89) T.F.Walsh, Phys.Lett. 36B, 121 (1971)
S.B.Brodsky, T.Kinoshita, and H.Terazawa,Phys.Rev.Lett.27,280(1971)
T.F.Walsh and P.Zerwas, Phys.Lett. 44B, 198 (1973)
E.Witten, Nucl.Phys. B 120, 189 (1977)
C.H.Llewellyn-Smith,Phys.Lett. 79B, 83 (1979)